This is to certify that the

thesis entitled

MODELING THE SORPTION OF WATER VAPOR
BY A SEMICRYSTALLINE POLYAMIDE:
APPLICATION OF A NEW INTERPRETIVE SORPTION MODEL

presented by

Kuniyoshi Ohashi

has been accepted towards fulfillment
of the requirements for

M.S. degree in Packaging

Major professor

Date 5/1/91

MODELING THE SORPTION OF WATER VAPOR BY A SEMICRYSTALLINE POLYAMIDE: APPLICATION OF A NEW INTERPRETATIVE SORPTION MODEL

By

Kuniyoshi Ohashi

A THESIS

Submitted to
Michigan State University
in partial fulfillment of the requirements
for the degree of

MASTER OF SCIENCE

School of Packaging

1991

ABSTRACT

MODELING THE SORPTION OF WATER VAPOR

BY A SEMICRYSTALLINE POLYAMIDE:

APPLICATION OF A NEW INTERPRETATIVE SORPTION MODEL

By

Kuniyoshi Ohashi

Experimental water sorption isotherm on nylon-6 was determined at 5°C, 23°C and 42°C. The sorption values were fitted by the modified dual-mode sorption model recently proposed by Hernandez et al. (1991). This model describes very well the data over a range of water activities from zero to one. The oxygen permeability behavior was studied as a function of polymer moisture content and it was shown that the oxygen permeability values decreased at low water activities and then increased with high water activities. DSC data showed that the percent crystallinity of nylon-6 increased with water content. The diffusion coefficient increased at low water activities and then decreased, but the solubility coefficient decreased at low water activities and then increased. Although the change in S and D are not conclusive, it appears that they may be associated with an increase in polymer crystallinity as water content increases within the polymer.

ACKNOWLEDGEMENTS

I gratefully thank my main advisor Dr. Ruben Hernandez, whose invaluable supports and criticisms guided me through every stage of this research. I would also like to thank Dr. Jack Giacin and Dr. E. A. Grulke for their precious advice, discussions, and help during this research.

I also thank Mr. Mike Rich, mainly from whom I learned to operate the DSC and DMA equipment, and Mr. Bob Hurwitz for helping me to make the apparatus of equilibrium sorption isotherm. I am deeply indebted to Suntory Limited which sent me to study in the School of Packaging. Finally, my foremost thanks go to my wife for the love and encouragement which made the completion of this thesis possible.

TABLE OF CONTENTS

LIST OF TABLES

LIST OF FIGURES

INTRODUCTION

It is well known that the presence of water molecules in a polymer can effect the permeability of oxygen through the polymer. Recently Hernandez et al. (1991) have studied the permeability of oxygen through an amorphous polyamide, nylon 6I/6T. This work led authors to propose a new model to describe the sorption of water vapor by the glassy polymer. The model is based on a Flory—Huggins and Langmuir sorption contributions given by

$$V_1 = V_1^L + V_1^{FH} \tag{1}$$

where V_1 is the total volume fraction of water within the polymer, and the superscripts L and FH refer to Langmuir and Flory—Huggins water sorption contributions, respectively. These contributions are expressed as:

$$V_1^L = \frac{K\ a_1}{1 + B\ a_1} \tag{2}$$

where K is the Langmuir capacity constant and B is the Langmuir affinity constant and

$$a_1 = \exp\left[\ln V_1^{FH} + (1 - V_1^{FH}) + \chi\,(1 - V_1^{FH})^2\right] \tag{3}$$

where a_1 is water activity, and χ is the Flory—Huggins interaction parameter. Equation (3) can be written in implicit form as:

$$V_1^{FH} = FH(a_1, \chi) \tag{4}$$

The proposed model was successfully used to explain the depression of oxygen permeability through the films as a function of sorbed water.

The newly developed Langmuir—Flory—Huggins model provided a more complete description of the sorption behavior of the water vapor—amorphous polyamide binary system. The model developed not only describes the sorption data, but also provides a correlation between used to evaluate the clustering function.

While the sorption of water vapor by polyamides has been reported, there is still the need for a systematic study of the equilibrium thermodynamics of the sorption process. This study also explains the mechanism of water sorption and its relationship with the transport and mechanical properties of purely amorphous and semicrystalline polyamides.

The objectives of this study are the followings:

1. Description of the sorption process for the binary system, water and semicrystalline polyamides nylon-6, and its relation to oxygen transport through the polymer.
2. Application of the newly developed Langmuir—Flory—Huggins model for interpreting the mechanism of sorption equilibrium of water vapor—semicrystalline polyamide system.

LITERATURE REVIEW

Chemistry Of Nylon-6

Nylons, or polyamides, are melt-processable thermoplastic materials whose chain structure features repeating amide groups. They offer a combination of properties that includes high strength (especially at elevated temperature), toughness at low temperatures, stiffness, wear and abrasion resistance, low coefficient of friction, and good chemical resistance (Carley 1991).

Nylon-6 is polymerized from e-caprolactam (6-carbons).

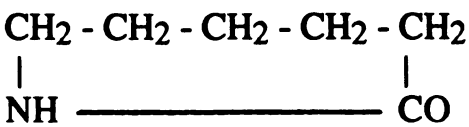

to form polycaproamide or nylon-6:

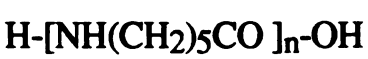

Crystal Structure Of Nylon-6

Crystal structure deals with the organization of long chain molecules into a microscopic array. If the array, on the average, is highly ordered in three dimensions, the material is said to have a high crystallinity. If the packing of the chains, averaged over the sample, is not very regular, the crystallinity is low. Nylons are different from many other semicrystalline

polymers such as polyethylene in that the degree of crystallinity of a given nylon can be controlled over a wide range of crystallinity. High crystallinity requires both parallel alignment of the chains and uniformity in the manner in which hydrogen bonds are formed (Clark and Wilson, 1973).

Crystallinity

A numerical measure of "crystallinity" is often used as a measure of the degree of crystalline order in a semicrystalline polymer. The term implies the presence of a two-phase system of crystalline and amorphous regions. This was a reasonable interpretation of the diffraction patterns of such polymers as polyethylene and polytetrafluoroethylene. Diffraction from these polymers resembles the superposition of a crystalline diffraction pattern on an amorphous pattern, which in turn appears to be an extrapolation of the diffraction pattern of the melt (Clark and Wilson, 1973).

For all the nylons there is no obvious procedure for resolution of a diffraction pattern into crystalline and amorphous regions and the calculation of even an empirical degree of crystallinity. There is no obvious demarcation between crystalline and amorphous areas (Satton, 1967). An instrument such as the Du Pont 310 curve analyzer can be used to resolve these patterns (Cambell, 1969) but the results can be quite arbitrary. Thus for polyamides, X-ray diffraction is not commonly used to derive a measurement of crystallinity (Clark and Wilson, 1973).

The usual methods for assessment of degree of crystallinity in nylons are by measurement of density, differential scanning calorimetry (DSC) or

by infrared techniques. Measurement of density is perhaps most satisfactory because it is rapid, precise, and unaffected by sample calibration - the assumption of amorphous and crystalline densities. It also requires close control over water content. The plasticizing effect of water on a dry sample of low crystallinity may increase its crystallinity . It should also be realized that massive samples are typically not uniform in crystallinity (Clark and Wilson, 1973).

The differential calorimetry scanning method for determining the percent crystallinity of a semicrystalline polymer is based upon the measurement of the heat of fusion, ΔH_f, and the reasonable assumption that this quantity is proportional to the percent crystallinity.(Wunderlich and Cromier, 1967). The percent crystallinity may be calculated from:

$$\text{Percent Crystallinity} = \frac{\Delta H_f}{\Delta H_f^*} \qquad (5)$$

where ΔH_f^* is the heat of fusion for a hypothetical 100% crystalline sample. For nylon-6, ΔH_f^* is 195 J/g (Brandrup and Immergut, 1991). Blatz (1989) measured the amount of crystallinity in 1 mil thick cast film of dry nylon-6, using DSC method and the percent crystallinity of that was 22%.

Infrared measurement of the intensities of crystalline and amorphous bands has been used as a measure of crystallinity and, when carefully done, correlates well with density measurements (Starkweather et al. 1956). For these studies, thin films were used so that the samples could be considered homogeneous.

Effect Of Crystallinity On Properties

The effect of crystallinity on the properties of nylon-6 is substantially the same as it is for other semicrystalline polymers. Modulus and strength and related properties such as hardness and yield point increase with increasing crystallinity. Measures of toughness such as impact strength decrease, particularly in the high-crystallinity range.

However, the effect of crystallinity can hardly be discussed independent of that of water. The properties of polyamides are as dependent on water content as they are upon crystallinity. The plasticizing effect of water on a dry sample of low crystallinity may increase its crystallinity. Not only can water have an effect on crystallinity, but it also changes physical properties independently. Once a sample has absorbed a given amount of water at any temperature, this water can be removed and replaced at this temperature without noticeable effect on crystallinity, but the effects in properties will be substantial. Water acts as a plasticizer for nylon-6 and lower the glass transition temperature and the characteristic temperatures of mechanical relaxation (Clark and Wilson 1973).

Glass Transition Temperature

Most polymers are either completely amorphous or have an amorphous-like component even if they are crystalline. Such materials are hard, rigid glasses below a fairly sharply defined temperature known as the glass transition temperature, Tg. At temperature above the glass transition temperature, at least at slow to moderate rates of deformation, the amorphous polymer is soft and flexible and is either an elastomer or a

very viscous liquid. Mechanical properties show profound changes in the region of the glass transition. Many physical properties change rapidly with temperature in the glass transition region. The importance of the glass transition temperature, Tg, in the mass transport of a penetrant-polymer system was described by Meares (1954), and is now very well recognized.

The glass transition temperature of any amorphous substance, whether polymeric or not, is defined as the point where the thermal expansion coefficient undergoes a discontinuity. In polymers, there may be more than one discontinuity in the thermal expansion coefficient. The largest discontinuity is usually associated with the loss of the molecular mobility which permits configurational rearrangements of the chain backbones; this is "the glass transition" (Ferry, 1970)

The sorption of gases above Tg indicates that the heat of solution must include along with the heat of interaction between the diffusant and polymer, the energy for separating the polymer chains which is endothermic, therefore accounting for the endothermic and slightly exothermic heat of solution. The exothermic heat of solution below Tg can be explained by the inclusion of the exothermic heat of adsorption for the "hole filling" in the heat of solution. The diffusion process above Tg requires a large zone of chain activation than below Tg which is consistent with the higher surge of activation reported above Tg (Hopfenberg and Stannet, 1973).

The glass transition temperature is generally measured by experiments which correspond to a time scale of seconds or minutes. If the experiments are done more rapidly so that the time scale is shortened , the apparent Tg is lowered. Thus, as generally measured, Tg is not a true

constant but shifts with time. (Nielson, 1974).

Blatz (1989) had measured the glass transition temperature of nylon-6 by using differential scanning calorimetry (DSC). However, no glass transition temperature could be determined for the nylon-6 because it is probably hidden in the crystallinity exotherm. According to Blatz, nylon-6 has a melting point (Tm) of 222°C and glass transition temperature (Tg) of 39°C. This Tg value of nylon-6 is reasonable from the relationship:

$$Tg / Tm \approx 0.6 \qquad (6)$$

The glass transition temperature of a nylon shifts to lower temperature as water contents is increased. The Tg of nylon-66 decreases from 80°C for an almost dry sample to 15°C for a sample saturated with water (Starkwether, 1973).

Relaxation Phenomena And Physical Properties

It is well known that increasing time and temperature have similar effects on viscoelastic properties (Tobolsky, 1960). Reliable estimates of the long-term properties of a polymer at a given temperature can be obtained from the short-term properties at higher temperatures. With a hydrophilic material, like nylon, the water content is an additional complementary variable. Increasing the water content has about the same effect as an increase in temperature or the time scale of the experiment (Starkweather, 1973).

In a time-temperature superposition, a time-dependent mechanical property, such as creep, stress relaxation, or dynamic mechanical loss is determined at a series of temperatures. The data for the various temperature are shifted along a log-time axis until they superimpose

(Starkweather, 1973). Quistwater and Dunell (1958, 1959) carried out a time-humidity superposition using filaments of nylon-66. The filaments were conditioned to various humidities, and forced longitudinal vibrations were applied at frequencies from 2 to 30 cycles per second. At 60°C, the maximum loss for the glass transition temperature occurred at 2% water, at 35°C, it was at 3.5% water, and at 9°C, it was at 6 to 8% water. It was concluded that the activation energy for the glass transition temperature is 60 to 80 kcal/mole.

Another study of time-humidity superpositions was reported by Onogi et al. (1962). They carried out measurements of stress relaxation on films of nylon-6 which had been treated at 150 to 155°C. Stress relaxation experiments were conducted in tension on dry samples at temperatures from 25 to 77°C. It was found that log-log curves of apparent modulus, E, versus time could be superimposed by shifting along the log-time axis for data taken at temperatures higher than 50°C. The shift factors correspond to an activation energy of 110 kcal/mole.

In another series of experiments, stress relaxation measurements were made at 25°C over a wide range relative humidities. At that temperature, relaxation was most rapid at 19 to 33% R.H., and the curves could be superimposed at those and higher humidities. For both time-temperature and time-humidity experiments, superposition was satisfactory only at conditions above the glass transition temperature (Starkweather, 1973).

The Association Of Water With Nylon

The effect of water on the properties of nylons has often been noted. The effect of crystallinity on the equilibrium water absorption of nylons was reported (Starkweather et al., 1973). Lowering the amide-group concentration and the relative humidity diminishes the effect of a change in crystallinity. There is little effect of temperature over nylon-6 and nylon-66, but a major effect is reported for nylon-11 at 100% R.H..

The dependence of equilibrium moisture content on relative humidity for typical moldings of commercial nylons was reported (Bonner et al., 1973). Nylon-6 reaches to equilibrium moisture content 10 wt % under the condition of 100% R.H..

The water absorption of modified composition obviously depends on the nature of the modification. Plasticized resin such as unextracted nylon-6 will have the same moisture content as extracted polymer but will show lower weight gain by virtue of loss of monomer. Even unmodified resins may contain about one percent of extractable material so that precise data will require a moisture analysis as well as weight gain information. On the other hand, resins containing glass or other inert additives absorb water in proportion to the fraction of nylon percent (Bonner et al., 1973).

Water has been shown to be a very effective plasticizer in certain amorphous and semicystalline linear polymers (Sauer and Lim, 1977). Similarly crosslinked polymers such as structural epoxy resins undergo a large depression in glass transition temperature when plasticized with small quantities (1-3 wt %) of water (Moy and Karasz, 1980). Because of the polar nature of water, and the hydrophilic nature of the polymers in which it is soluble, specific interactions in the form of disruptive hydrogen

bonding of water molecules to polar sites on the polymer chains have been invoked to explain these large effects. Indeed, several spectroscopic (Banks and Ellis, 1979) and calorimetric (Ellis and Karasz, 1984) studies of epoxy resins plasticized by water have suggested that specific interactions may be present. However, a recent NMR study of an epoxy resin plasticized by water has clearly indicated that water molecules have a large degree of mobility, which tends to negate any argument that water molecules become specifically and firmly "bound" to be very good groups in the polymer (Jelinski et. al., 1983).

The plasticization of semicrystalline polymers, such as that of nylon-6 by water, has attracted considerable attention (Fuzek, 1980). The nylon-6/water system also has an additional complexity in that unlike an amorphous network, where plasticizer is assumed to be distributed homogeneously throughout the polymer, the water will reside principally in the noncrystalline regions. It has previously been noted (Beatty and Karasz, 1975) that in some semicrystalline polymers, the incremental change in heat capacity at the glass transition temperature (Tg) does not obey a simple quantitative two-phase relationship, and is substantially reduced, as the degree of crystallinity increases.

The influence of crystallinity and crosslinking on the depression of the glass transition temperature in nylon-6 by water was investigated by dynamic mechanical methods (Jin, X. et. al., 1984). The study had attempted to quantitatively account, both theoretically and experimentally, for the water-induced plasticization behavior of nylon-6 of different crystallinity and proposed nylon-6 to be described by a three-phase model: a fully ordered crystalline phase, a bulk amorphous phase which is not capable of activation at Tg and is therefore unable to contribute to the

incremental change in heat capacity at this transition. Although it is clear that the interpretation of plasticization studies from semicrystalline polymers is considerably complicated by morphological factors, there appeared to be good agreement between the theoretical and experimental depression of the glass transition temperature in nylon-6 by water . Regarding the analogy between the effect of crystallinity on thermal properties and the influence of chemical crosslinking on those a network polymer, it is probable that the influence of morphology and the concomitant distribution of plasticizer in the amorphous region is of greater significance in determining the plasticization behavior of this semicrystalline polymer.

Puffr and Sabenda (1967) suggested a mechanism of water sorption into nylon-6 at room temperature, which involved two neighboring amide groups in water-accessible regions forming a sorption center. This sorption center could accommodate up to 3 water molecules, involving hydrogen bonding between adjacent amide groups. Additional sorbed water molecules may be accommodated via a clustering mechanism.

Papir et al. (1972) investigated the relaxation behavior of nylon-6 as a function of orientation, anisotropy and moisture content by using an inverted free-oscillating torsion pendulum and three new relaxations were discovered. The characteristics of these new relaxations strongly depend on the orientation anisotropy and concentration of adsorbed water in the specimens. The results suggested that motions of the polar groups, in addition to those of the methylene sequences, are involved and two types of water, tightly bound and loosely bound, exist in nylon-6.

Hernandez et al. (1991) studied Fourier Transform Infrared (FTIR) spectroscopy to detect possible charges in hydrogen bonding between N-H

and carbonyl group by observing the vibrational modes of the amide group, using amorphous polyamide. FTIR data suggest that the water does not change the hydrogen-bonding strength of the carbonyl group but does change the hydrogen bonding strength of the N-H group.

The Permeation Mechanism For Gases Through Polymers

Steady state rate of permeation of gases through a polymer is usually described by the permeability coefficient (P). The permeability coefficient (P) can be determined from direct measurement of the rate of transfer of a gas through a polymer or from the relationship:

$$P = D^*S \qquad (7)$$

where D and S are separately determined (Crank and Park, 1968). D is the diffusion coefficient which describes the rate of movement of a diffusing permeant through the polymer, and S is the solubility coefficient of the permeant in the polymer.

Mass transport through polymers occurs by a diffusion process rather than by a flow process such as Knudsen or Poiseuille flow that occurs through porous materials (Lebovitz, 1966). The diffusion process is affected by the characteristics of the polymer, diffusant gases, the temperature and the relative humidity. Therefore, if permeation is to occur, the permeant gas has to undergo the following processes in succession: (i) dissolution of the penetrant molecule into the surface of the polymer film: (ii) diffusion of the penetrant molecule through the polymer matrix; and (iii) desorption of the permeant molecule from the other surface of the film (Lebovitz, 1966).

The diffusion process can take place because polymer molecules have a random kinetic agitation or heat motion. The polymer chain segments have vibrational, rotational and translational motions that continually create temporary "holes" in the polymer matrix. The creation of these holes allows penetrant molecules to move trough the polymer matrix under the influence of the concentration gradient. The amplitude and motion of

the polymer molecules is directly related to the temperature, chemical composition and morphology of the polymer.

The glass transition temperature (Tg) is important factor for the mass transport of a penetrant-polymer system (Meares, 1954). The glass transition temperature marks the transition from a "glassy" polymer state to a "leathery" polymer state. This increases flexibility of the polymer is causes by the unfreezing of micro brownian motion of polymer chain segments 20-50 carbon atoms in length (Boyer, 1977). This increase in polymer chain segmental mobility above the glass transition temperature corresponds with an increase in permeability and diffusion.

Small diffusant molecules like the permanent gases: oxygen, nitrogen and carbon dioxide, have almost no effect on the polymer molecules while sorbed into the polymer matrix. Their kinetic agitations are rapid compared to those of the polymer chains. The rate of diffusion of these molecules is therefore controlled by their agitation which is related to the amount of energy present in the system, as measured by the temperature. If a concentration gradient is present across a film the frequency of the jumps of the diffusant past the polymer chains gives a net flux of the diffusant molecules through the film (Meares, 1965).

As stated above, permeability is related to diffusion and solubility. The complex permeability process is best understood by considering the effects of various factors on solubility and diffusion. This portion of the text on the characteristics of permeation and diffusion of gases through polymer membranes follows from the excellent review in the chapter on Permeability and Chemical Resistance by C. E. Rogers from the book "Engineering Design for Plastics" edited by E. Baer (1964).

Solubility Characteristics

The solubility of a molecule component in a solid can be described as the distribution of the component between two or more phases. The uptake of penetrant by a solid is called sorption and can be considered to have adsorption or absorption as the basic mechanism. There is no way of distinguishing between either physical adsorption and chemisorption or considered a composite of these various modes.

The dependence of the solubility coefficient on temperature generally follows an Arrhenius type relationship:

$$S = S_0 \exp(-\Delta H_S/RT) \qquad (8)$$

where ΔH_S is the apparent heat of solution (Rogers, 1964). The process of sorption by a polymer may be considered to involve two stages: condensation of vapor onto the polymer surface followed by solution of the condensed vapor. The heat of solution can be expressed as the sum of the molar heat of condensation (ΔH_C) and the partial molar heat of mixing (ΔH_1). The heat of mixing is always positive and the heat of condensation can be positive or negative depending on whether the molecule is a gas or vapor. For permeant gases, ΔH_S is slightly positive so that S increases slightly with temperature. However for the more condensable vapors (like organic compounds), ΔH_S is negative due to the relatively large heat of condensation, thus the solubility decreases with increasing temperature.

A sorption isotherm is a curve that relates the equilibrium concentration of the penentrant in the polymer (c), to the concentration of penetrant (p) surrounding the solid, at any constant temperature. There are classically four basic types of isotherms observed in polymer systems.

These isotherms depend on the degree of penetrant-polymer interaction. Type I follows Henry's law where the concentration is linearly dependent upon pressure. Type II is characteristic in systems where only a unimolecular layer of sorbed substance forms on the substrate showing a concave curve towards the pressure axis. Type III sorption is characteristic of multilayer adsorption where the attractive forces between penetrant and solid are greater than those between the molecules of the penetrant themselves, giving a sigmoid shaped curve. When the forces between the penetrant and the substrate are relatively small, the sorption process occurs essentially randomly as the results of absorption or adsorption due to van der Waals type forces. The resulting isotherm corresponds type IV. Type IV sorption forms a convex curve towards the pressure axis.

Another interpretation of the type III isotherm considers that it is the result of two simultaneously sorption process. One process, dominant at low penetrant concentrations, corresponds to a type II isotherm due to preferential sorption of penetrant onto a limited number of active sites in the solid.

The other concurrent process is a type IV sorption, so the superposition of the two curves gives the observed type III isotherm.

The solubility coefficient at a given permeant partial pressure can be calculated from these sorption isotherms by dividing the sorbed concentration (c) by the corresponding pressure (p) (Rogers, 1964). The Langmuir (1918) equation for sorption limited to monolayer formation leads to a type II isotherm. The Langmuir equation can be expressed as:

$$S = \frac{c}{p} = \frac{C'_H p}{1 + b p} \qquad (9)$$

where b is the hole affinity constant, C'_H is the hole saturation constant.

The Langmuir equation works best when the energies of adsorption are high, as in chemisorption, or when the adsorbed molecules are quite large. In both cases, the penetrant molecules are rendered relatively immobile by the adsorption process. However, at high concentrations or low temperatures, discrepancies often appear in the direction of more sorption than predicted by the Langmuir equation. This is especially apparent when the energies of adsorption are in the range characteristic of physical adsorption. These discrepancies may be due to the formation of multilayers rather than momolayers.

The BET equation, which accounts for such multilayer adsorption, was originally derived by Brunauer et al. (1938) on the assumption that the Langmuir equation could be applied to each layer. In the usual form of the BET equation is different from that for the subsequent layers. The adsorbed penetrant from the second layer on is assumed to be equal to the heat of vaporization for the pure liquid penetrant.

The expression for the solubility coefficient in terms of readily measured concentrations and vapor pressure is:

$$S = c/p = \frac{\beta c_m}{(p^0 - p)\{1 + (\beta-1)(p/p^0)\}} \qquad (10)$$

where: p^0 is the permeant saturated vapor pressure

c_m is the sorbed concentration of vapor corresponding to a complete monolayer sorption

$\beta = \exp(Q_1-Q_L / RT)$ where Q_1 is the heat of adsorption for the first layer, Q_L is the heat of vaporization for the pure liquid penetrant.

The BET equation in this form can predict isotherms of types II, III, and IV depending primarily on the relative magnitudes of Q_1 and Q_L. When $Q_1 >> Q_L$, corresponding to strong attractive forces between the first layer and the substrate, the BET equation approximates the Langmuir equation and type II isotherm. On the other hand, when $Q_1 < Q_L$ a type IV isotherm results. Intermediates cases, $Q_1 > Q_L$, leads to sigmoid isotherm curves: it is for these type III isotherms that the BET equation has been most used.

The magnitude of the solubility for a penetrant in a polymer increases with : (i) the chemical similarity of the penetrant-polymer; (iii) the larger the molar volume of the condensed penetrant; and (iv) the lower the percent crosslinking and the crystallinity of the polymer. The sorption of penetrant by the polymer has a profound effect on the solid properties. In addition to the plasticizing action of the sorbed penetrant there may be changes in the polymer structure due to swelling and distortion incurred during sorption as well as actual chemical attack on the polymer (Rogers, 1964).

Models For Polar Systems At High Solute Activities

Solute sorbed at temperatures below their boiling point (such as water at room temperature) may not obey simple and ideal phase equilibria relations such as Henry's law. For these cases, eqn. (10) does not describe the data well over the activity range, $0 < a_1 < 1$, and usually

underpredicts the actual solubility values at high activities. This lack of agreement has been explained as a "positive deviation" of the Henry's law caused by the swelling of the polymer network as the penetrant is sorbed.It is postulated that the network swelling exposes more binding sites and increases the sorption level of the penetrant synergistically (Vieth et al., 1976).

Berens (1975) reported that the Flory-Huggins equation adequately described data for vinyl chloride/poly(vinyl chloride). for high molecular weight polymers, the Flory-Huggins expression is :

$$\ln a_1 = \ln V_1 + V_2 + \chi V_2^2 \qquad (11)$$

where χ is the interaction parameter. Although eqn. (11) does not provide the most accurate description of the thermodynamic performance of polymer solutions, it does contain most of the essential features which distinguish such solutions (Prausnitz et al., 1986). Eqn. (11) usually fits equilibria data over a wider range than Henry's law. For example, sorption data of toluene in polyvinyl chloride is well fit by the Flory-Huggins equation especially for $0.5 < a_1 < 1.0$ (Berens, 1985). Sfirakis and Rogers (1980) studies the sorption of vapors by nylon-6 but did not present a mathematical model to describe the sorption process. However, this data set can be fit to eqn. (11) with a χ value of 1.88. The Henry's law term seems adequate for fitting the water/kapton data (Yang et al., 1985). Either hole filling or chemisorption might be occurring in the polyimide for the Langmuir contribution, as kapton is known to hydrogen bond with water. Water is known to hydrogen bond with a variety of epoxies and the dual mode sorption model describes some data well (Barrie et al., 1984).

Diffusion Characteristics

The temperature dependence of diffusion coefficients over small temperature ranges at a constant vapor concentration can be represented by an Arrhenious type relationship:

$$D = D_0 \exp(-E_D / R T) \quad (12)$$

where E_D is the apparent activation energy for the diffusion process. The activation energy for diffusion is associated with the energy required for "hole" formation in the polymer matrix plus the energy required to move the molecule through the polymer structure. The pre-exponential factor ,(D_0), can be thought of as being related to the frequency and magnitude of the holes or "looseness" within the polymer microenvironment in the absence of penetrant. The activation energy of the polymer increases at temperatures above the polymer's glass transition temperature.

The magnitude of the concentration dependence of diffusion in any given polymer is dependent on the temperature, molecular size, chemical similarity between penetrant and polymer and the penetrant concentration in the polymer. The solubility coefficient is often essentially constant at low vapor activities for the more volatile vapors while the diffusion coefficient exhibits significant concentration dependence. The concentration dependence of the diffusion coefficient can be represented by the equation :

$$D = D_0 \exp(\gamma c) \quad (13)$$

Where γ is a characteristic constant, D_0 is a pre-exponential factor representing the diffusion coefficient at zero concentration or the limiting diffusion coefficient and c is the concentration of permeant in the polymer.

The diffusion coefficient may deviate significantly from a linear or

exponential dependence on c when the measurements are made over wide temperature ranges and vapor concentration, or activity, especially with more easily condensable vapors. Such behavior has been observed for allyl chloride in polyvinylacetate; for n-acetates in polymethylacrylate; and for hydrocarbons in polyethylene (Meares, 1958ab; Fujita, 1961; Rogers, 1960). The concentration dependence in theses systems can be represented by a simple exponential function of vapor activity:

$$D = D_0 \exp(\alpha a_1) \qquad (14)$$

where α is a constant and a_1 is the vapor activity on the high concentration side of the film .

The magnitude of D_0 depends primarily on the chemical nature, size, and shape of the penetrant and the morphology of the polymer. The constants γ and α can be interpreted as characterizing the effectiveness of various penetrants to plasticize a polymer and to facilitate its segmental mobility.

The addition of a plasticizer to a polymer usually, but not always, increases the rate of gas and vapor diffusion and permeation (Boyer, 1949). An increase in transport rate is probably due to an increase in polymer segmental mobility resulting from a decrease in the cohesive forces between chains by replacement of polymer-polymer contacts by polymer-plasticizer contacts. this is reflected by the observed decrease in activation energy for diffusion with increasing plasticizer content.

Additional complications for an accurate prediction of plasticizing action arise from the lowering of the glass transition temperature, enhanced rates of stress relaxation, and gross morphological changes induced by the addition of a plasticizer itself also may be an important factor affecting the overall solubility and transport rate, especially at high

plasticizer contents (Boyer, 1949).

Ideal Diffusion And Sorption

Diffusion is the net transport of matter in a system by means of random molecular motion. This results in the removal of chemical potential differences in a system and eventually produces a uniform state of equilibrium if the boundary conditions are not held constant for a permeation experiment.

Frequently the rate of diffusion is proportional to the concentration gradient although the proportionality constant known as the diffusion coefficient may be a function of the diffusant concentration in the polymer:

$$J = -D(c)\ \frac{\partial C}{\partial x} \qquad (15)$$

where D is the concentration independent diffusion coefficient of the fixed gas in the polymer, and C is the concentration of fixed gas in the polymer. This is Fick's first law of diffusion and is found experimentally to represent diffusion in many systems. For gases above their critical temperature (fixed gases) the diffusion coefficient is not a function of concentration. Fick's second law may be derived from Fick's first law:

$$\frac{dc}{dt} = \frac{\partial}{\partial x}\left[D(c)\frac{\partial c}{\partial x}\right] \qquad (16)$$

Diffusion which follows Fick's first and second laws is termed Fickian diffusion (Hopfenberg and Stannet, 1973)

Non-ideal Sorption And Diffusion

The magnitude of the negative enthalpies of sorption reported by Meares (1958) for neon, nitrogen, oxygen and argon in glassy polyvinylacetate and by Barrie et al. (1957) for organic vapors in ethyl cellulose were inconsistent with the sorption theories of rubbery systems and led Barrie to suggest a two-mode, concurrent sorption mechanism for glassy polymers, namely ordinary dissolusion and "hole" filling (Hopfenberg and Stannet, 1973).

Michaels et al. (1963) also reported that the sorption of helium, nitrogen, oxygen, argon and methane in glassy, amorphous and glassy, crystalline polyethylene telephthalate for pressure up to 10 atmosphere obeyed Henry's law, but carbon dioxide at 25°C and 40°C and ethane at 25°C in the same pressure range derived from Henry's law. The carbon dioxide isotherms promoted Michaels et al. (1963) to propose a dual-mode sorption model of ordinary dissolution and adsorption in microvoids (holes) for gas sorption in glassy amorphous polymers. It was assumed that the total amount of solute sorbed in the polymer, C, consisted of two thermodynamically distinct molecular populations:

$$C = C_D + C_H = K_D\, p + \frac{C'_H\, p}{1 + b\, p} \qquad (17)$$

where C_D and C_H are the solubilities due to absorption and adsorption. The concentration C_D was represented by Henry's law:

$$C_D = K_D\, p \qquad (18)$$

where K_D is the Henry's law constant.

The concentration C_H was represented by a Langmuir isotherm:

$$C_H = \frac{C'_H\, p}{1 + b\, p} \qquad (19)$$

Modified Dual Mode Sorption Model

Hernandez et.al.(1991) have proposed to modify eqn. (17) by using the Flory-Huggins equation to describe non-specific solution rather than Henry's law. The modified dual-mode sorption model represents the sorption of water vapor by an amorphous polyamide at 23° C. This modification allowed the model to fit over the activity range, $0 < a_1 < 1$. For convenience, the modified dual mode sorption model was expressed in terms of volume fractions and solute activity:

$$V_1 = V_1^{FH} + V_1^{L} \qquad (1)$$

where V_1^{FH} refers to the Flory-Huggins contribution to the solute volume fraction and V_1^{L} is Langmuir volume fraction contribution. Since eqn. (11) is nonlinear, the value for V_1^{FH} was determined by numerical methods, such as the Newton-Raphson technique and eqn. (1) became:

$$V_1 = FH\,(a_1, \chi) + \frac{K\, a_1}{1 + B\, a_1} \qquad (20)$$

where $K=C'_H\, f b p_s$, $B=b p_s$, p_s is the saturation vapor pressure of the solute and f is a conversion factor.

The Effect Of Crystallinity On Sorption

The effects of the degree of crystallinity on the permeability of semicrystalline polymers was first discussed by Michaels and Parker, and

Michaels and Bixler have extended this study to the effect of crystallinity on the sorption of several gases in rubbery, crystalline polyethylene, and found that solubility constants for a particular gas were proportional the amorphous volume fraction, that is:

$$k = \alpha k^* \tag{21}$$

where k* is the solubility constant of a hypothetical completely amorphous polyethylene and k is the solubility constant of partially crystalline polyethylene. This relationship suggested that the gases sorb entirely in quantity sorbed was directly proportional to α (Hopfenberg and Stannet, 1973).

The relationship in equation (21) was used by Michaels, Vieth and Barrie (1963) in studying the effect of crystallinity on the sorption of several gases in glassy crystalline polyethyleneterephthalate. Unlike the rubbery crystalline polyethylene, it was found that the gas solubility, with the exception of helium, is not directly proportional to amorphous volume fraction. The decrease in solubility accompanying crystallization was smaller than the corresponding reduction in amorphous volume fraction.

This result can be satisfactorily accounted for in terms of the "hole" model of glassy amorphous phase. Upon annealing the polymer it is more probable that the denser regions crystalize first, tending to remove more of amorphous phase used for gas dissolution, therefore leaving the residual amorphous phase with a higher concentration of "holes" than in the previously amorphous polymer. This means that crystallization in glassy polymers tends to increase the relative contribution of "hole" filling. Also such an increase in concentration of "holes" with increasing crystallization accounts for the decreases reductions in solubility (Hopfenberg and Stannet, 1973).

Michaels et al.(1963) generalized their original dual sorption model to include the effects of crystallinity on the solubility of the dissolved species:

$$C = \frac{C'_H\, b\, p}{1 + b\, p} + \alpha k^*_D\, p \qquad (22)$$

EXPERIMENTAL METHODS

Nylon-6 film

Allied-Signal Inc. P. O. Box 2332R Morristown, NJ 07963 CAPRAN 77C 1.25 MIL CAPRAN 77C is a transparent, durable, nylon-6-type thermoplastic film made from a polymer of e-caprolactam. An all-purpose packaging-grade film, approved in accordance with FDA regulations.

Equilibrium Sorption Data

Equilibrium sorption data was taken on polymer films using a Cahn Electrobalance Model 2000 (Cahn Instruments Inc. Cerritos, California). A stream of nitrogen adjusted to specific values of water activity provided the source of water vapor in equilibrium with the polymer films. The film samples were dried under vacuum at 70° C before each run. The electrobalance was maintained a constant temperature environment (5° C, 23° C and 42° C) in the Temperature Humidity Test Chamber (Thermotron Model SM-32S-SH, Thermotron Industries, Holland Michigan). The temperature tolerance is ±0.3°c. A sample film approximate 100 mg was normally used for equilibrium sorption data, and the sensibility of the apparatus was around 1 microgram. A schematic diagram of the test

system is shown in Figure 1. The test system allows for the continuous collection of sorption isotherm data of water vapor by a nylon-6 film from the initial time zero, when the film is first exposed to the vapor, to the steady state condition, when sorption equilibrium is reached. As shown, the nylon-6 film sample to be tested was suspended directly from one of arm of the electrobalance and a constant concentration of penetrant vapor was continually flowed through the sample tube (hang-down tube), such that the sample film was totally surrounded by the vapor. A constant concentration of permeant vapor was produced by bubbling nitrogen gas through distilled water. This was carried out by assembling a vapor generator consisting of a glass gas washing bottle containing the water, and a fritted dispenser tube. The concentration obtained in this way was adjusted to a required value by mixing it with a pure nitrogen gas stream. Water activities were measured using Hygrometer Sensors (Hygrodynamic Co., Silver Spring, Maryland). The vapor generator system and humidity senser were mounted in the constant temperature chamber (Thermotron). As shown, flowmeters were used to provided a continuous indication that a constant rate of flow was maintained. Gas flow was regulated using needle valves. The gain in weight of the sample due to penetrant sorption was monitored continually until the gain was zero at equilibrium. .

Oxygen Permeability Studies

These studies were carried out on an Ox-Tran 100 Permeability Tester (Modern Controls, Inc., Elk River, Minnesota). This apparatus was modified to allow the two streams, oxygen and carrier gas, to be adjusted to specific water vapor activities. An schematic of the modified

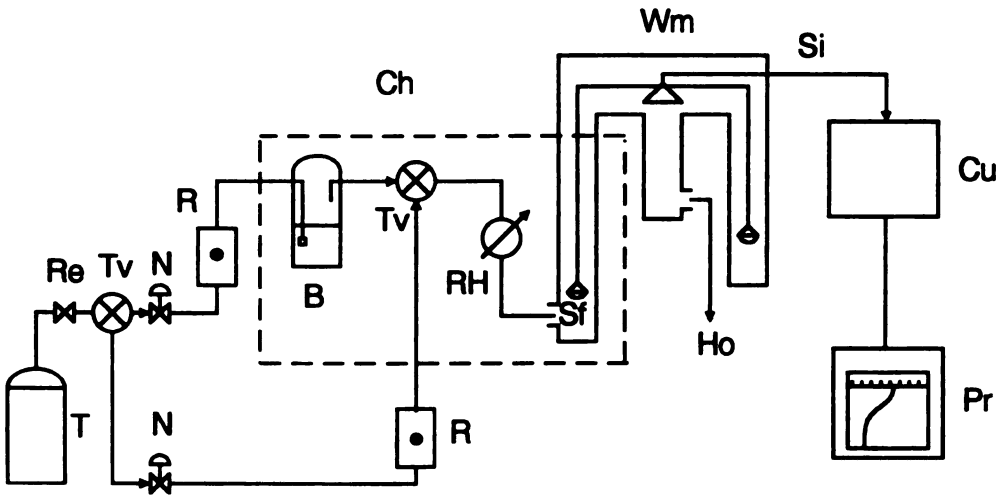

B - Water Bubbler
Ch - Temperature Constant Chamber
Cu - Control Unit
Ho - Hood
N - Needle Valve
Pr - Printer
RH - Humidity Sencer
R - Rotameter
Re - Regulator
Sf - Sample film
Si - Electric signal
T - Nitrogen Tank
Tv - Three way Valve
Wm - Cahn Electrobalance

Figure 1. Schematic diagram of the electrobalance test apparatus

apparatus is shown in Figure 2 (Hernandez et al., 1991, IAPRI preceedings). As shown, each stream is formed by mixing a wet and dry gas component to obtain the required activity value. Water activities were measured using Hygrometer Sensors (Hygrodynamic Co., Silver Spring, maryland). Sample films were dried under vacuum at 70° C before each run. The equilibration process between the Nylon-6 film and the gas phase, at selected values of water activities, was carried out with the sample film mounted into the permeation cell. The required time to reach equilibrium was previously determined by gravimetric method, using the Cahn electrobalance. Although time consuming, this procedure avoided sample handling and assured correct conditions of test. The experiments were conducted at three different temperature (5° C, room temperature and 42° C). When the tests of 5° C and 42° C, whole system were run in the temperature controlled chamber.

Differential Scanning Calorimetry Experiments

The Differential Scanning Calorimetry (DSC) experiments were performed on a DuPont 9000 Thermal Analyzer (E. I. DuPont De Nemours & Co., Inc. Wilmigton, Delaware). Film samples were placed in small aluminum pans and vacuum dried at 70° C. Samples were then equilibrated over salt solutions to give selected water vapor activities at room temperature. Polyethylene closed containers with salt solution provided selected values of water vapor activities and samples were placed in the containers until they reached equilibrium. After reaching equilibrium, the aluminum pans containing film samples were placed in glass vials to maintain the conditions and then were carried to the DSC

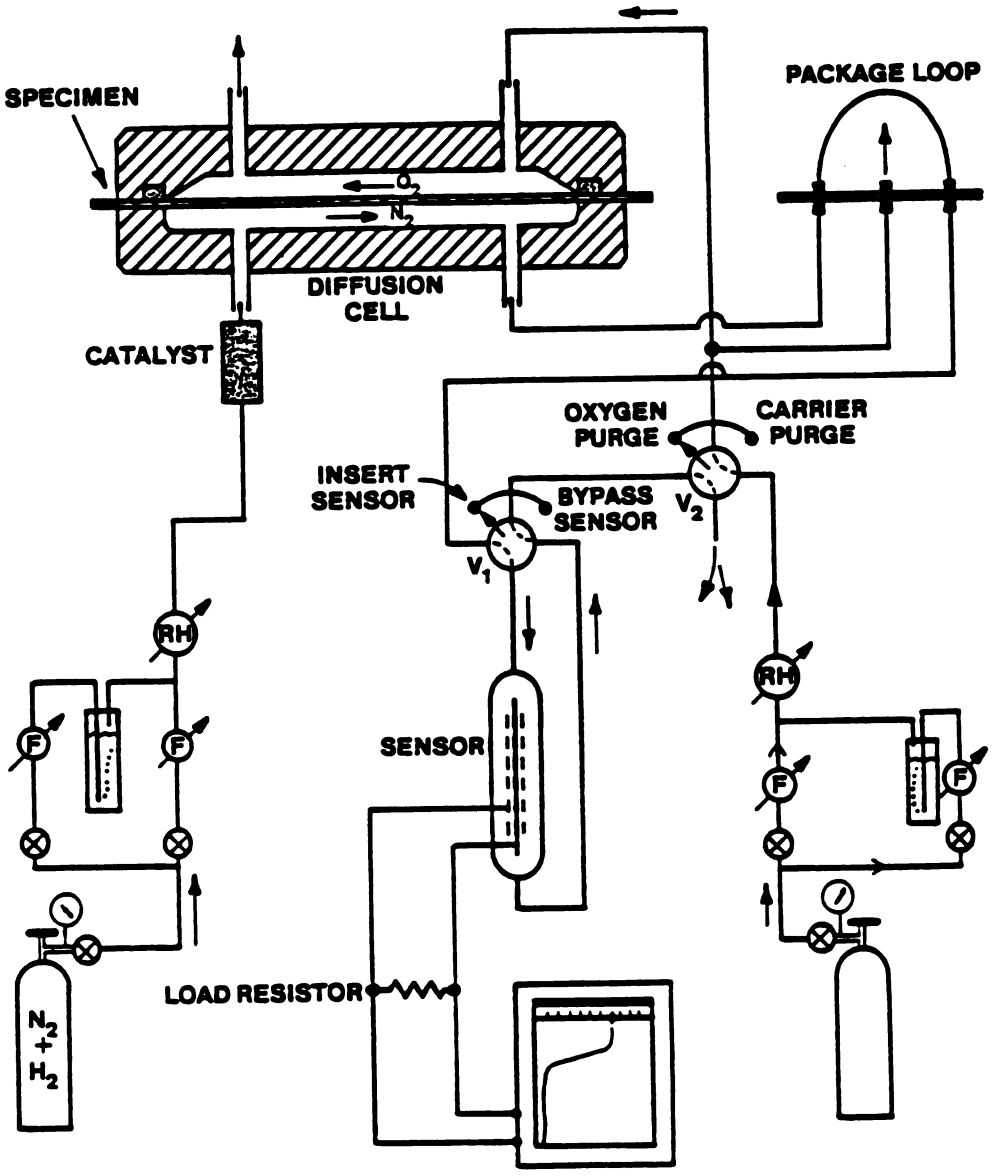

Figure 2. Oxygen permeability apparatus

equipment. The differential scanning calorimeter was programmed for the heating rate of 10° C/min and the heating temperature range of room temperature to 250 ° C with approximately 10 ~ 15 mg of sample film in each run.

RESULTS AND DISCUSSION

Equilibrium Sorption Isotherm

Sorption equilibrium values of water weight fraction in the nylon-6 film at 5°C, 23°C and 42°C are presented in Table 1. Isotherm data was obtained over a wide activity range (especially low water activity) in order to provide a good test of the modified dual model. Figure 3 shows the sorption isotherm for water in nylon-6 at 5°C, 23°C and 42°C. As expected, the solubility of water in the polymer decreases when temperature increases. The apparent sigmoid shape may be described by the Langmuir-Flory-Huggins model, given by eqn. (20).

Figure 4 shows the experimental sorption values and Flory-Huggins fitting at 23°C. The solid curve through the data is the Flory-Huggins equation (eqn. 11) with χ value of 1.846. The value of interaction parameter was calculated by using computer program prepared by Dr. R. J. Hernandez based on a Box-Kanamazu modification of Gauss method of minimization of sum of squares for nonlinear models (Hernandez et al. 1991). This model represents the data at high water activities well, but underestimates the data at low water activities. Figure 5 shows the experimental sorption values and Flory-Huggins fitting at low water activity. A linear regression method was used to determine the parameter values estimated for eqn. (20). A computer program was used to determine the constants of eqn. (20), χ, B and K. Starting with the value

Table 1. Equilibrium sorption isotherm experimental data

Temperature 5°C		Temperature 23°C		Temperature 42°C	
Water Activity	Weight Fraction	Water Activity	Weight Fraction	Water Activity	Weight Fraction
0.000	0.0000	0.000	0.0000	0.000	0.0000
0.069	0.0068	0.067	0.0055	0.040	0.0033
0.130	0.0120	0.096	0.0074	0.09	0.0069
0.182	0.0147	0.148	0.0108	0.120	0.0087
0.260	0.0202	0.182	0.0126	0.148	0.0098
0.370	0.0289	0.238	0.0162	0.23	0.0151
0.440	0.0350	0.306	0.0206	0.370	0.0235
0.650	0.0533	0.380	0.0257	0.50	0.0302
0.950	0.0893	0.470	0.0312	0.540	0.0332
		0.520	0.0350	0.595	0.0369
		0.650	0.0454	0.735	0.0460
		0.790	0.0587	0.87	0.0616
		0.840	0.0652		

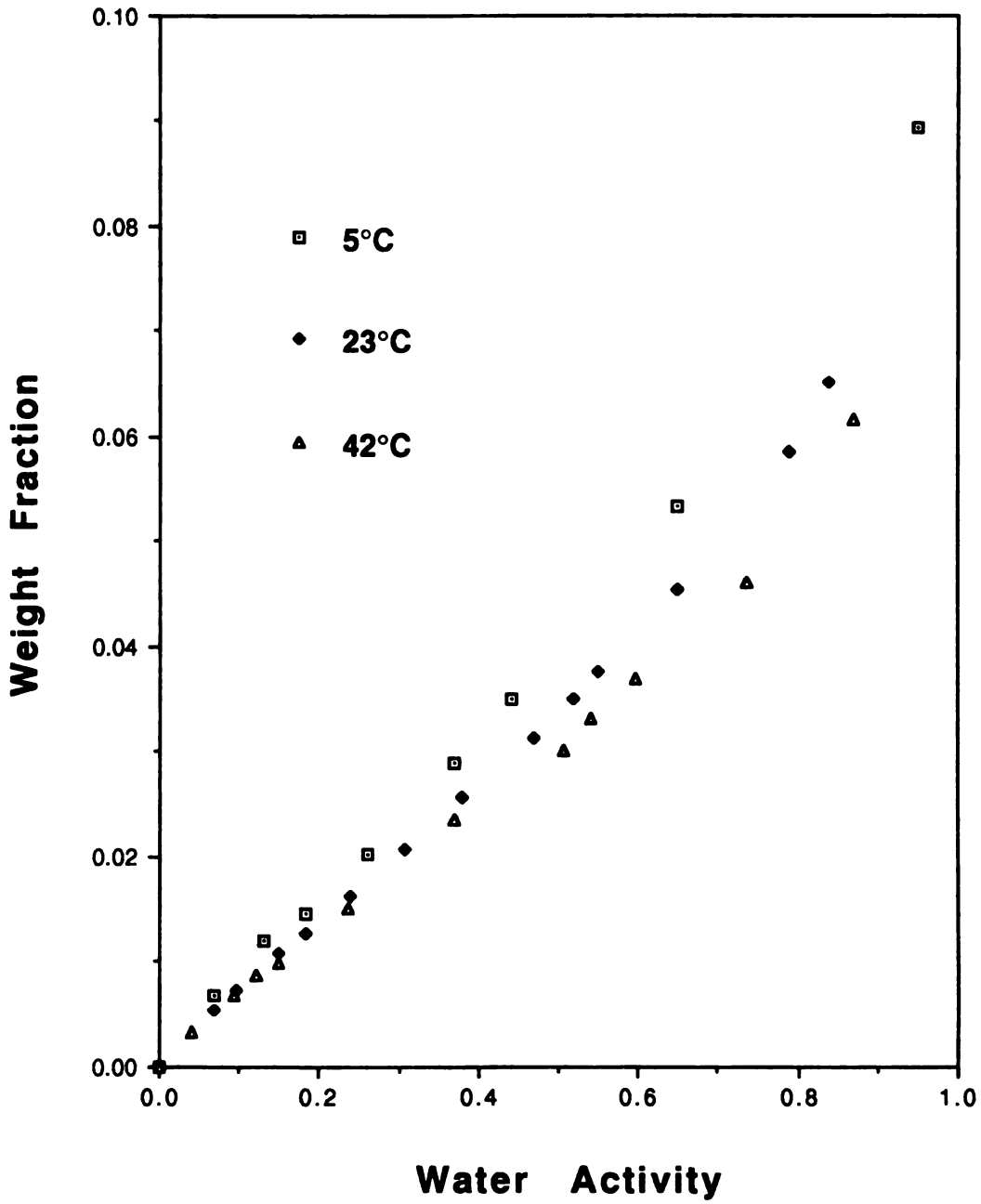

Figure 3. Water sorption isotherm at 5°C, 23°C and 42°C

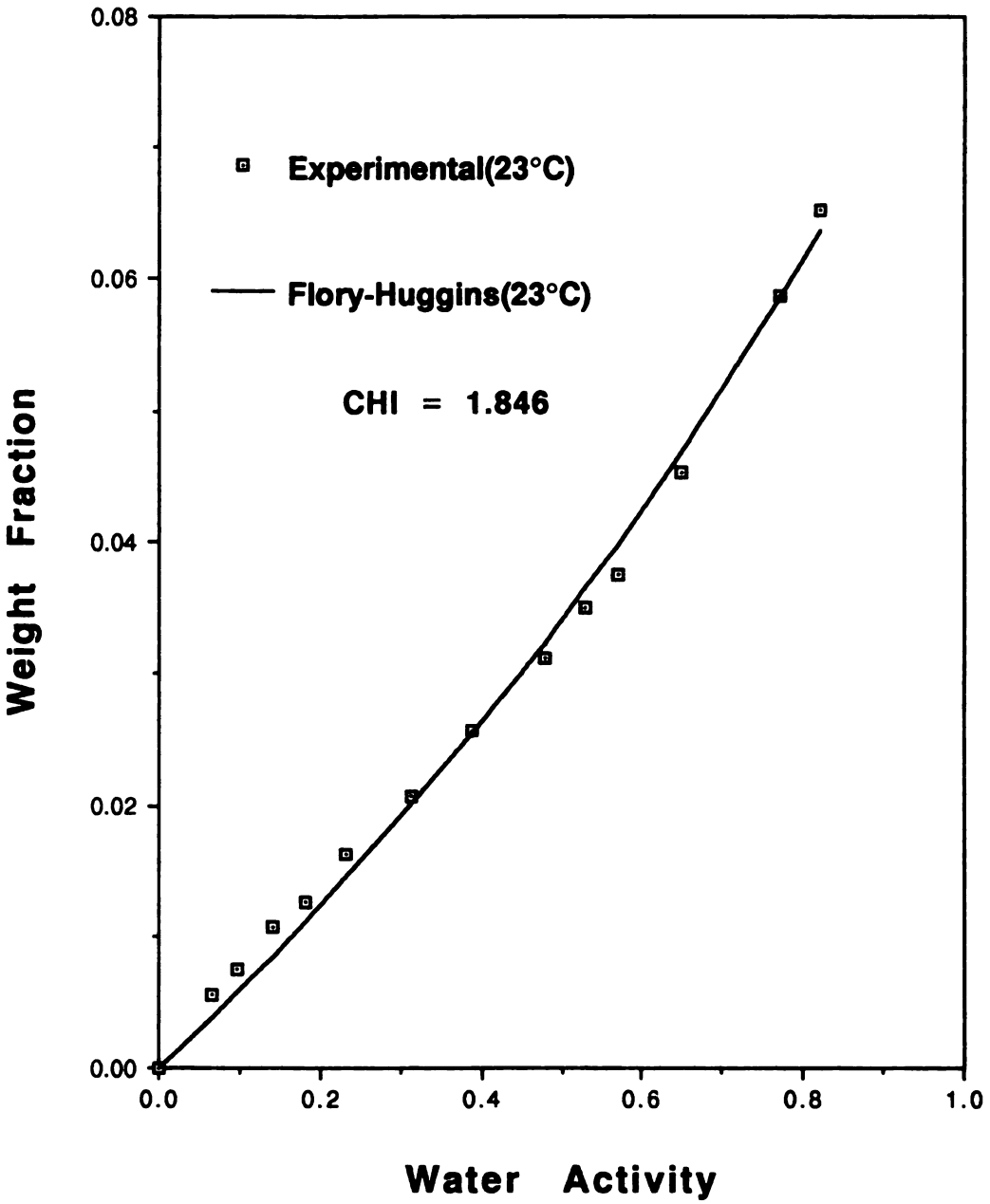

Figure 4. Experimental sorption values and Flory-Huggins fitting at 23°C

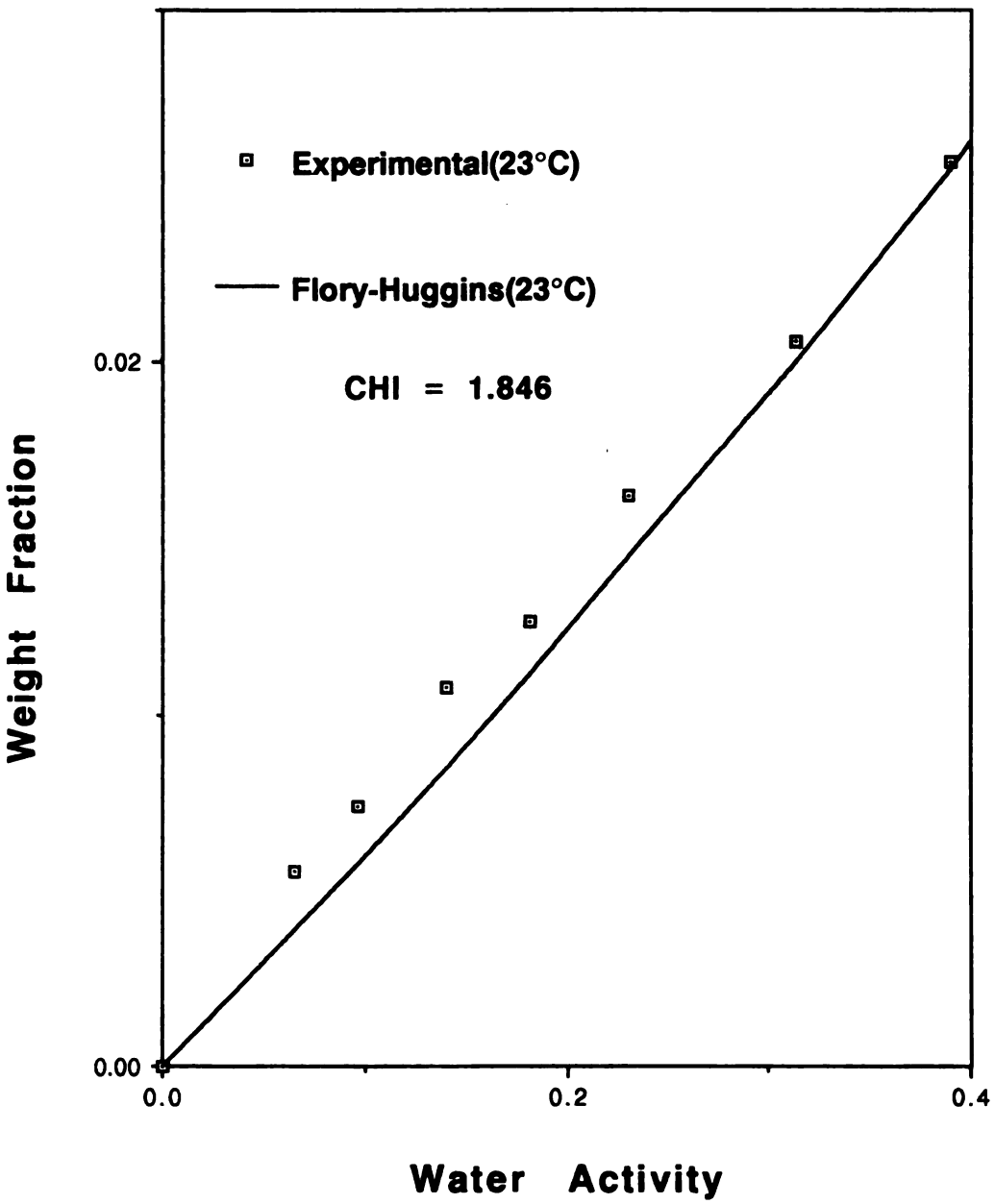

Figure 5. Experimental sorption values and Flory-Huggins fitting at low activity values

of χ calculated by the Box-Kanamazu method, the program calculated K and B by a linear regression analysis of the following equation converted from the Langmuir equation (9):

$$\frac{1}{V_1^L} = \frac{1}{K} + \frac{B}{K}\frac{1}{a_1} \qquad (22)$$

where V_1^L is expressed as following equation:

$$V_1^L = V^{exp} - V^{FH} \qquad (23)$$

where V^{exp} is the experimental data and V^{FH} is the Flory-Huggins value. For a series of χ values, the sum of squares of the difference between the experimental and calculated value were calculated. The values of χ, B and K were then associated with the minimum value of sum of squares. Sum of squares were plotted as a function of χ to find the best estimates of the parameters. Figure 6, 7 and 8 show the sum of squares versus χ at 5°C, 23°C and 42°C respectively. The χ values of the minimum of each convex curve should be the best estimate of the parameters for each temperature.

Table 2, 3 and 4 show the contribution of Langmuir and Flory-Huggins factors over the activity range at 5°C, 23°C and 42°C respectively, using the parameters shown in figure 6, 7 and 8. At low activities, the Langmuir contribution is relatively high compared to the Flory-Huggins contribution. Figure 9, 10 and 11 present Langmuir curves calculated by the computer program as a function of water activity at 5°C, 23°C and 42°C respectively. The difference between experimental and Flory-Huggins values (eqn. 23) were plotted through the Langmuir curve. These plots are relatively close to the Langmuir curve. The Langmuir contribution is nearly constant at activities greater than 0.1. The

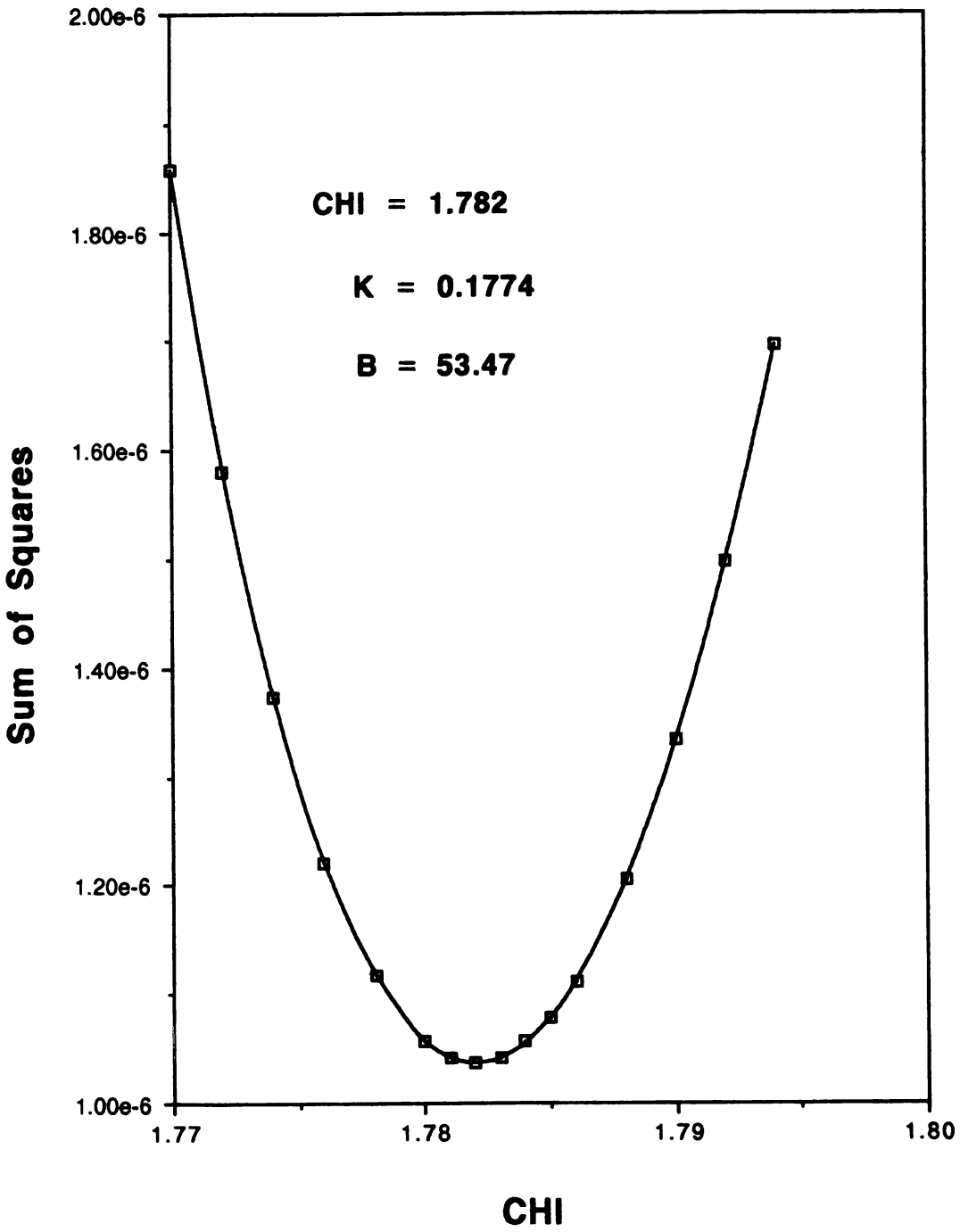

Figure 6. Sum of squares versus CHI at 5°C

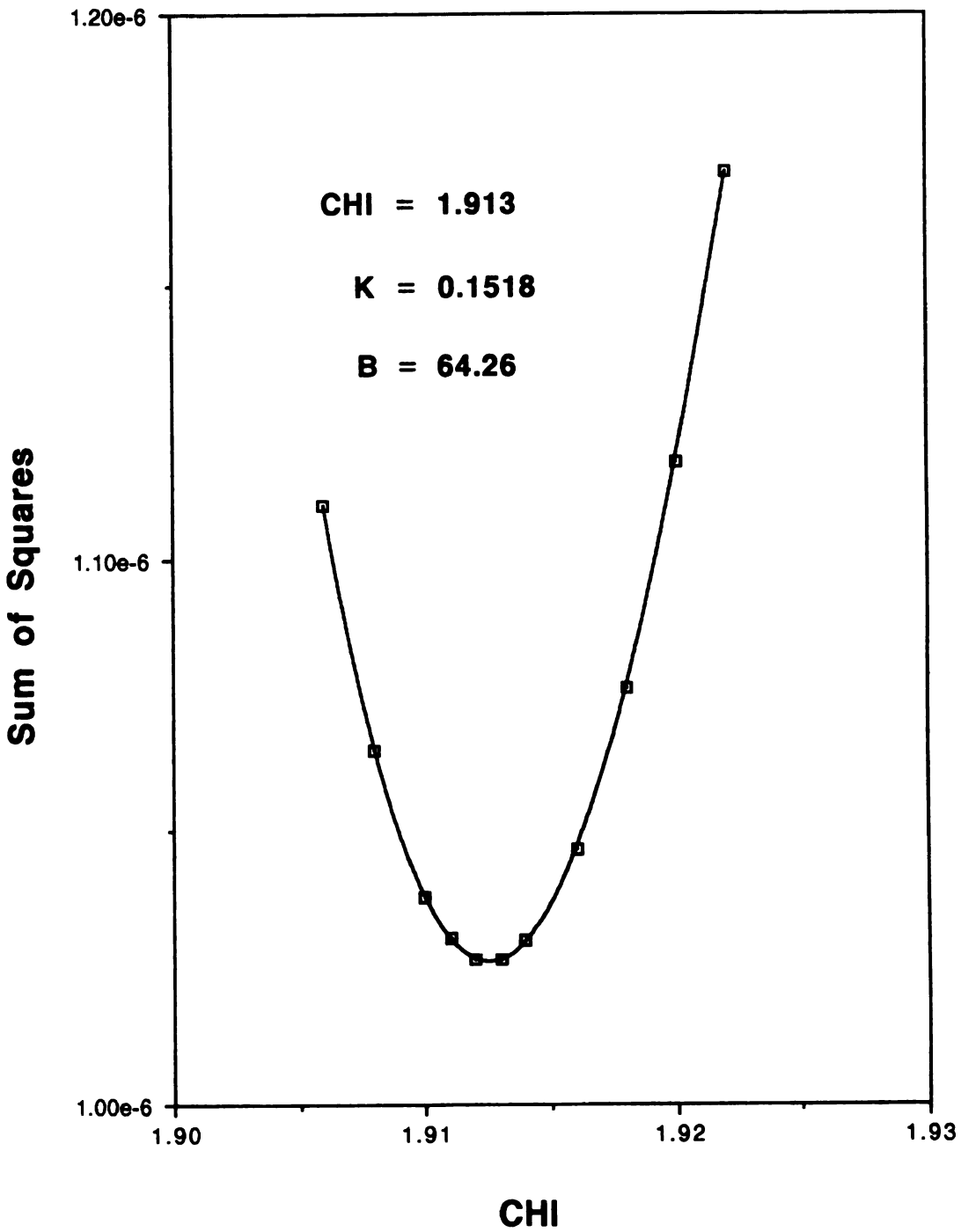

Figure 7. Sum of squares versus CHI at 23°C

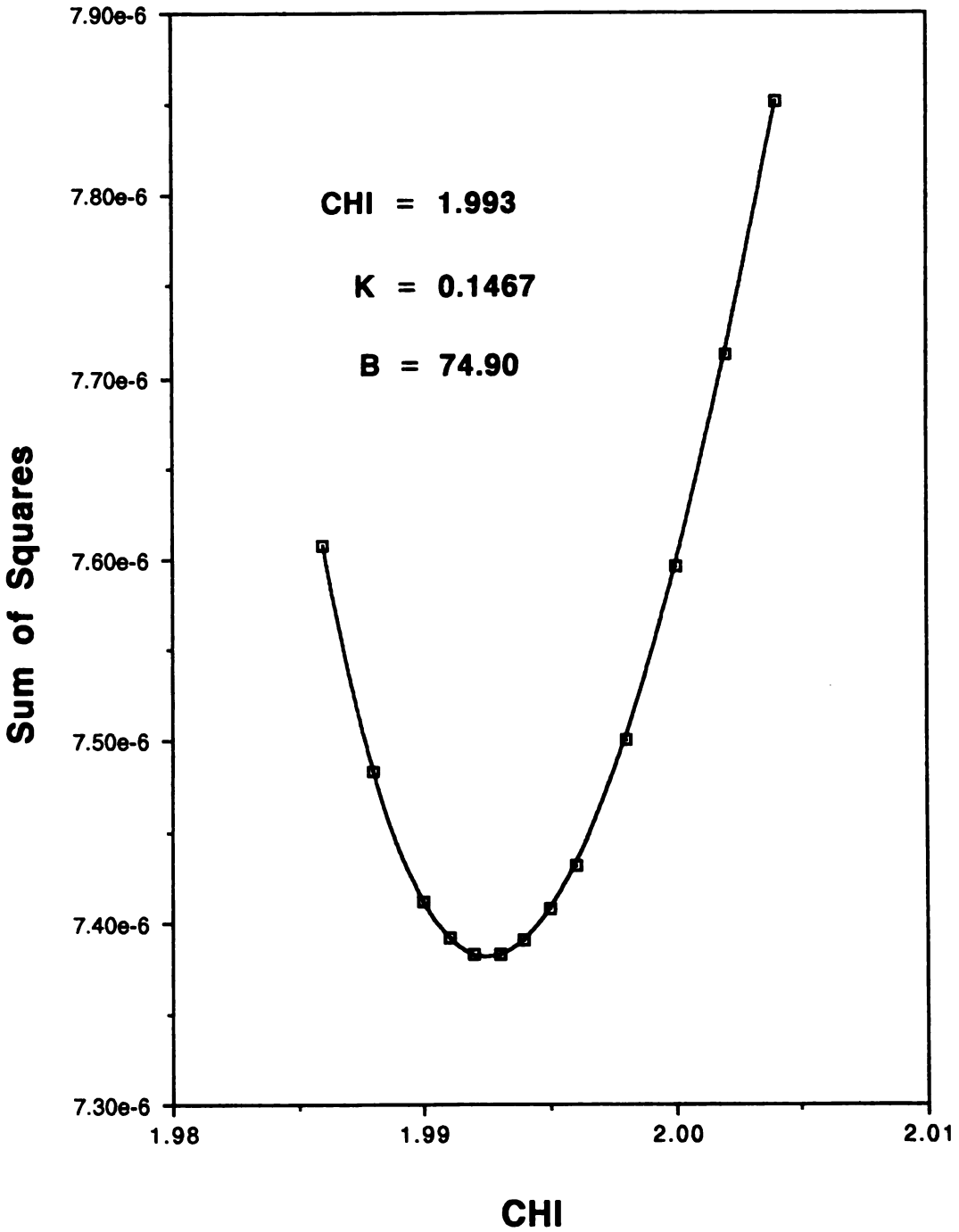

Figure 8. Sum of squares versus CHI at 42°C

Table 2. Langmuir and Flory-Huggins weight fraction contributions

Temperature = 5°C

CHI = 1.782

K = 0.1774

B = 53.47

Water Activity	Langmuir	F-H	Total
0.0	0.0	0.0	0.0
0.069	2.610E-03	4.358E-03	6.967E-03
0.130	2.900E-03	8.361E-03	1.126E-02
0.182	3.001E-03	1.189E-02	1.490E-02
0.260	3.094E-03	1.742E-02	2.051E-02
0.370	3.157E-03	2.573E-02	2.889E-02
0.440	3.182E-03	3.138E-02	3.456E-02
0.650	3.224E-03	5.043E-02	5.366E-02
0.950	3.253E-03	8.592E-02	8.918E-02

Table 3. Langmuir and Flory-Huggins weight fraction contributions

Temperature = 23°C

CHI = 1.913

K = 0.1518

B = 64.26

Water Activity	Langmuir	F-H	Total
0.0	0.0	0.0	0.0
0.067	1.916E-03	3.704E-03	5.621E-03
0.096	2.032E-03	5.350E-03	7.382E-03
0.148	2.136E-03	8.368E-03	1.051E-02
0.182	2.175E-03	1.039E-02	1.257E-02
0.238	2.217E-03	1.381E-02	1.603E-02
0.306	2.225E-03	1.812E-02	2.037E-02
0.380	2.269E-03	2.304E-02	2.531E-02
0.470	2.286E-03	2.936E-02	3.165E-02
0.520	2.293E-03	3.306E-02	3.535E-02
0.550	2.296E-03	3.533E-02	3.764E-02
0.650	2.306E-03	4.337E-02	4.567E-02
0.790	2.316E-02	5.584E-02	5.816E-02

Table 4. Langmuir and Flory-Huggins weight fraction contributions

Temperature = 42°C

CHI = 1.993

K = 0.1467

B = 74.90

Water Activity	Langmuir	F-H	Total
0.0	0.0	0.0	0.0
0.092	1.711E-03	2.026E-03	3.494E-03
0.120	1.763E-03	6.205E-03	7.968E-03
0.148	1.797E-03	7.710E-03	9.507E-03
0.236	1.854E-03	1.260E-02	1.445E-02
0.370	1.891E-03	2.053E-02	2.242E-02
0.505	1.908E-03	2.924E-02	3.115E-02
0.540	1.912E-03	3.163E-02	3.355E-02
0.595	1.916E-03	3.552E-02	3.744E-02
0.870	1.929E-03	5.780E-02	5.973E-02

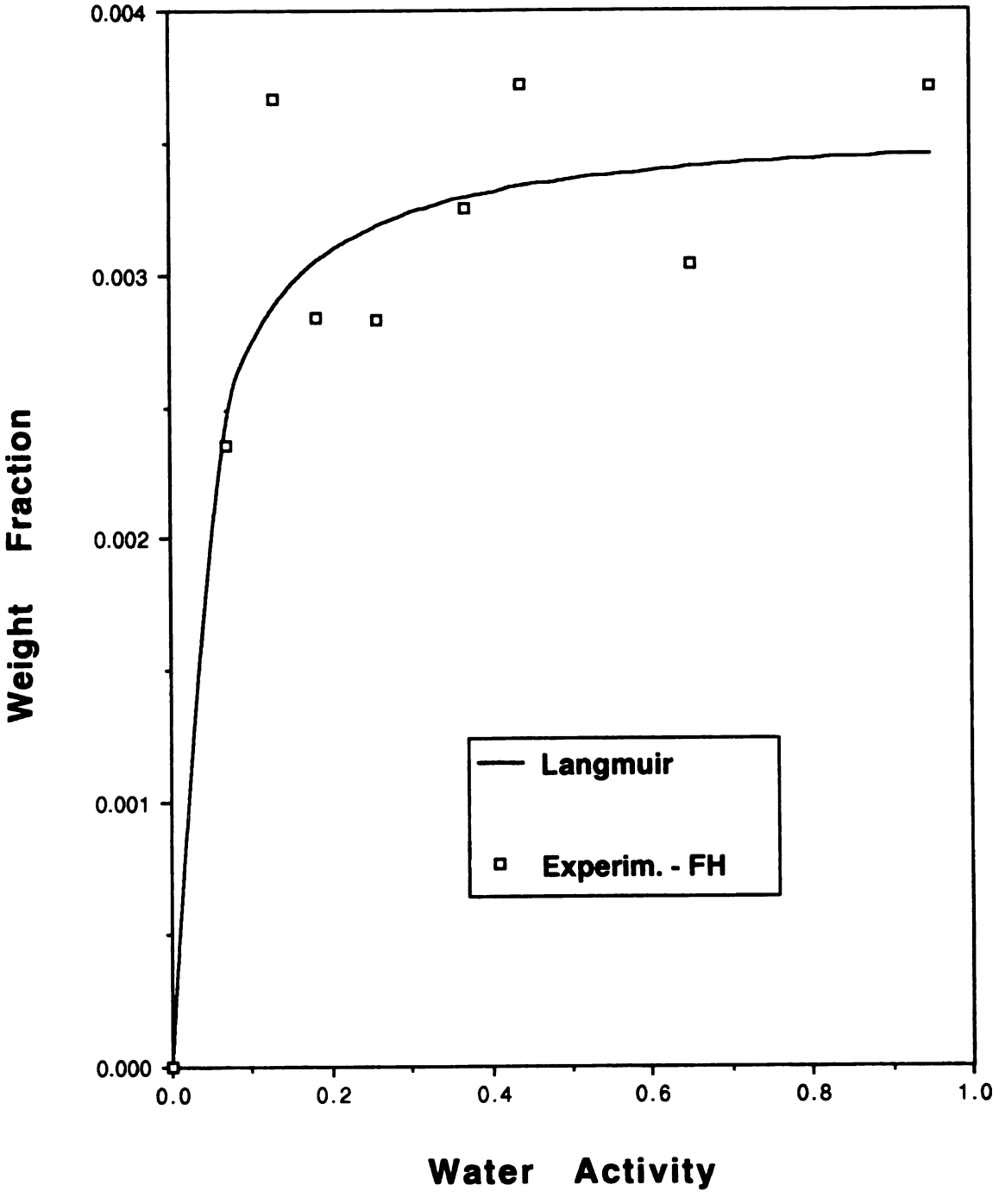

Figure 9. Langmuir plot at 5°C

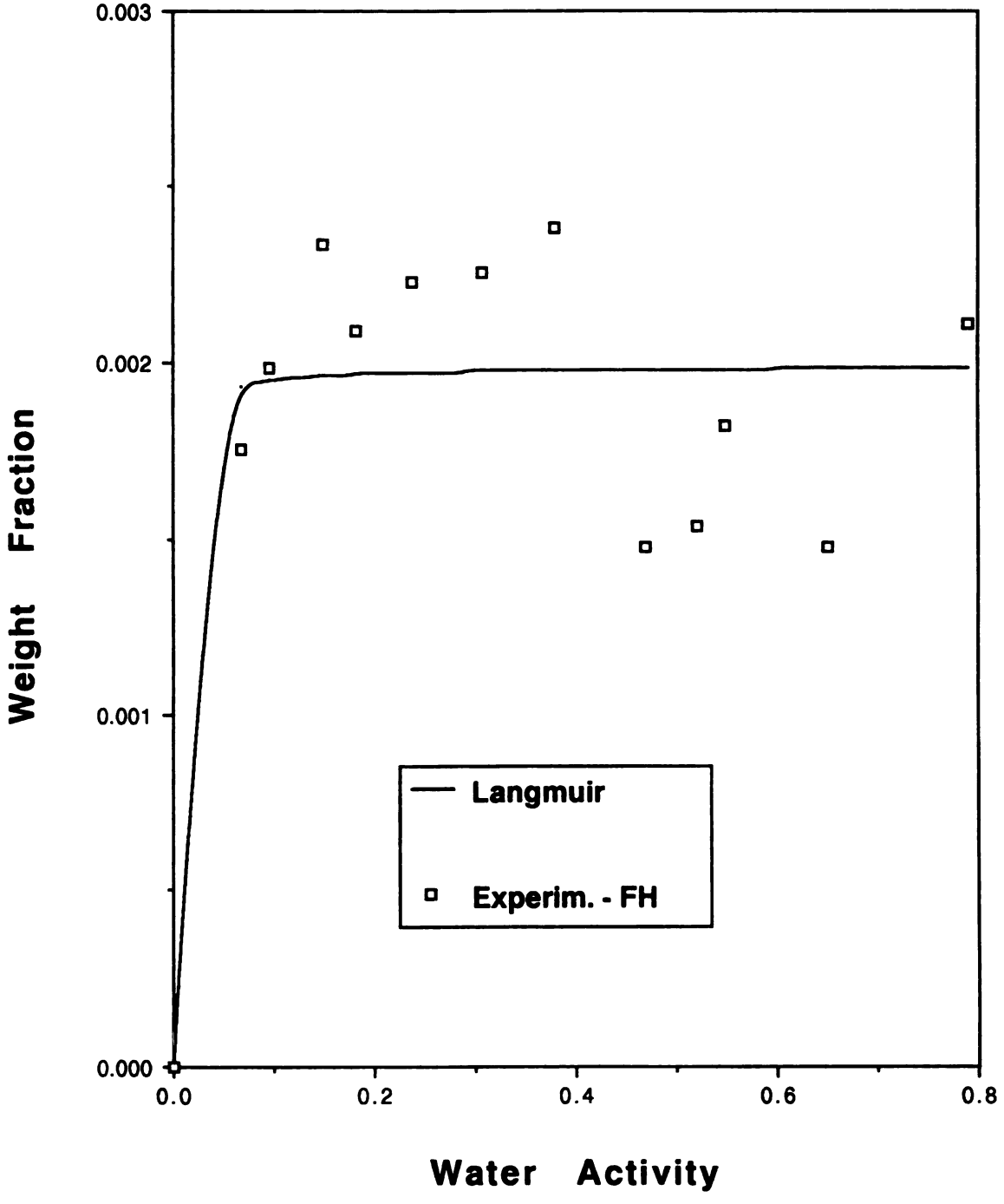

Figure 10. Langmuir plot at 23°C

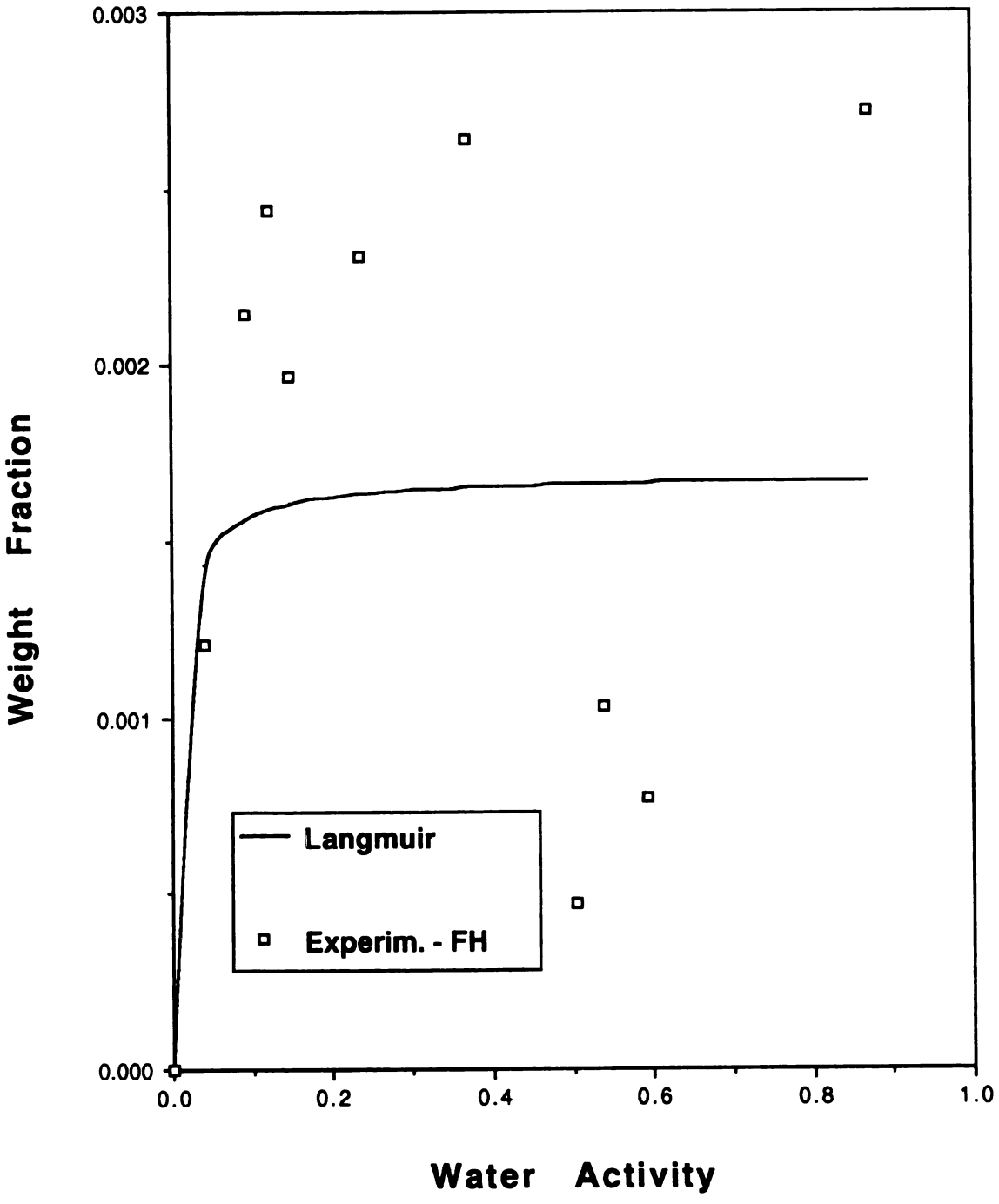

Figure 11. Langmuir plot at 42°C

points of water activity value 0.84 at 23°C and 0.735 at 42°C were eliminated when the linear regression method was calculated, because these points were too far from Langmuir curve. Experimental errors such as the instrumental error of humidity sensers must have happened at these points.

Figure 12, 13 and 14 show eqn. (9) as the solid curve of best fit for Langmuir-Flory-Huggins model and the complete data set at 5°C, 23°C and 42°C respectively. The Langmuir-Flory-Huggins model presented by Hernandez et al. (1991) describes accurately the sorption of water by nylon-6 as well as amorphous polyamide, over a broad range of water activity. The initial Langmuir contribution suggests the presence of a limited number of sorption sites which are immediately available to water molecule and following broad extent may be indicative of clustering or multi-layer formation (Kawasaki et al., 1962) at the higher water activity.

Table 5 shows the values for χ, K and B at 5°C, 23°C and 42°C. K value decreases as temperature increases, but on the other hand, χ and B value increase when temperature increases. The Arrhenius plots of K and B are presented in Figure 15 and 16 respectively. There are good linear relationship between 5°C and 42°C in both Arrhenius plots. The following expression correlate the constants K and B as a function of temperature:

$$K = 3.54E\text{-}02 * \exp(442/T) \quad (25)$$

$$B = 957 * \exp(-801/T) \quad (26)$$

Oxygen Permeability

Tables 6, 7 and 8 present the values of permeability, diffusion coefficient and solubility of oxygen in nylon-6 at 5°C, room temperature

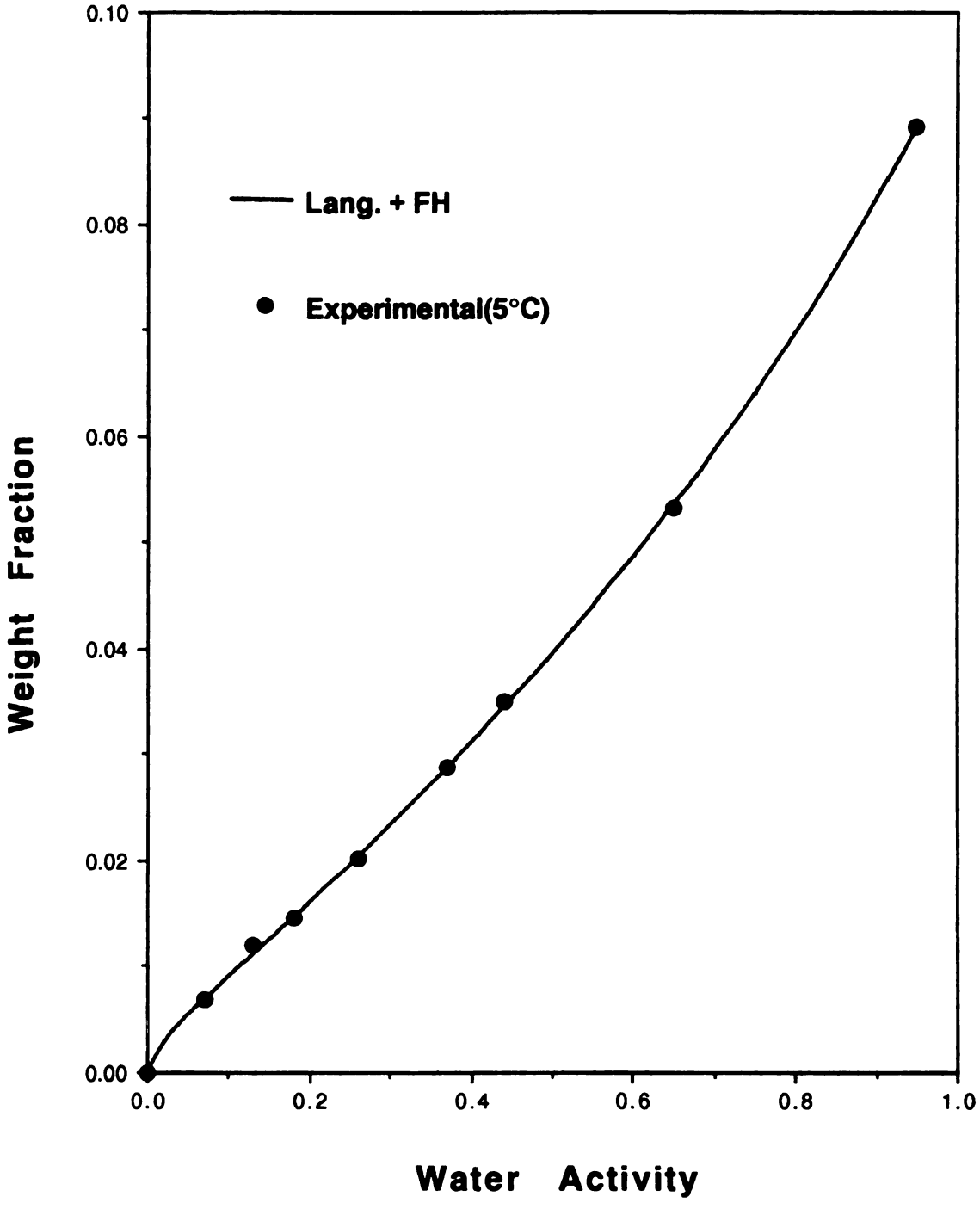

Figure 12. Best fit for the Langmuir-Flory-Huggins model

Values of parameters are CHI=1.78, K=0.177 and B=53.5

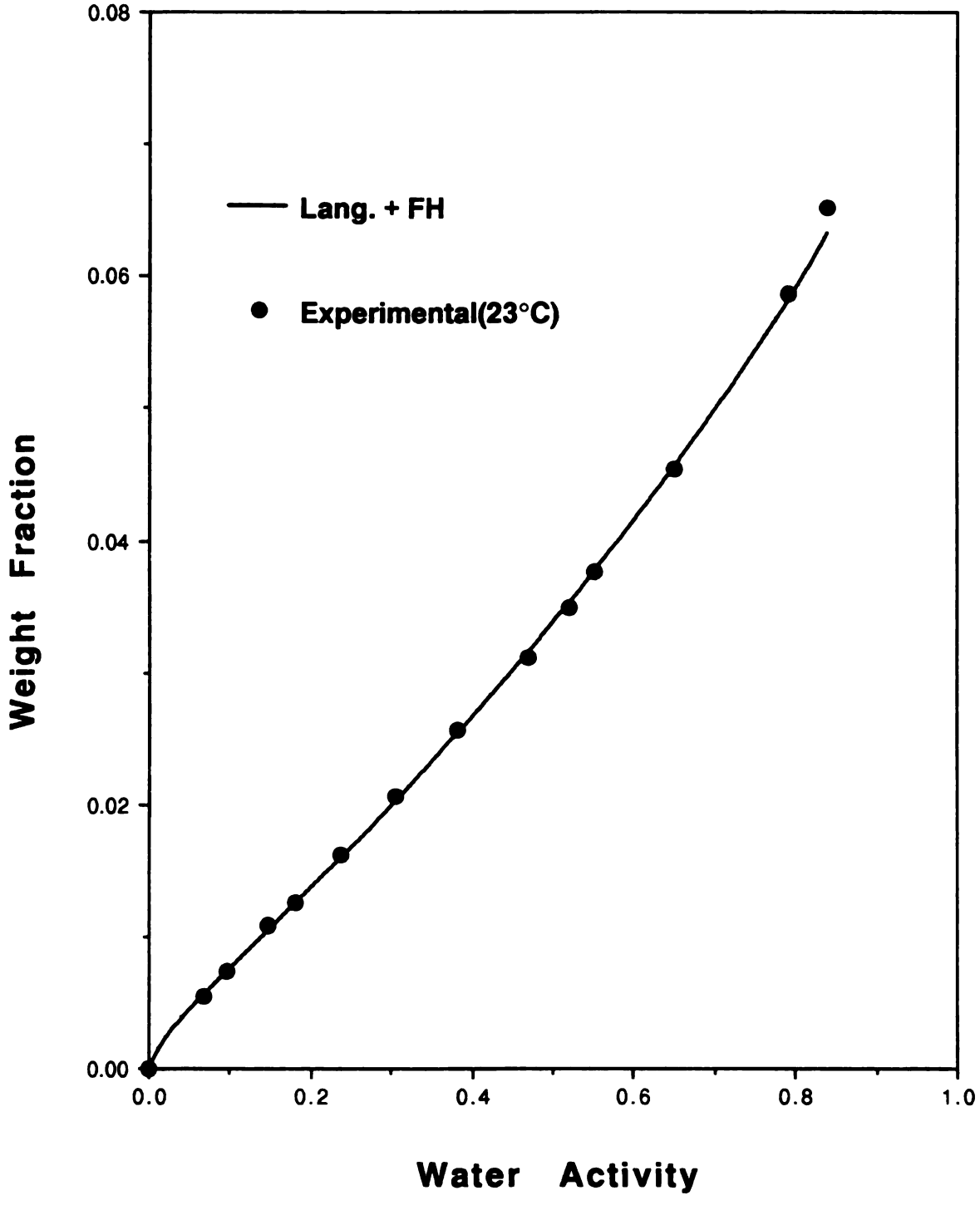

Figure 13. Best fit for the Langmuir-Flory-Huggins model

Values of parameters are CHI=1.91, K=0.152 and B=64.3

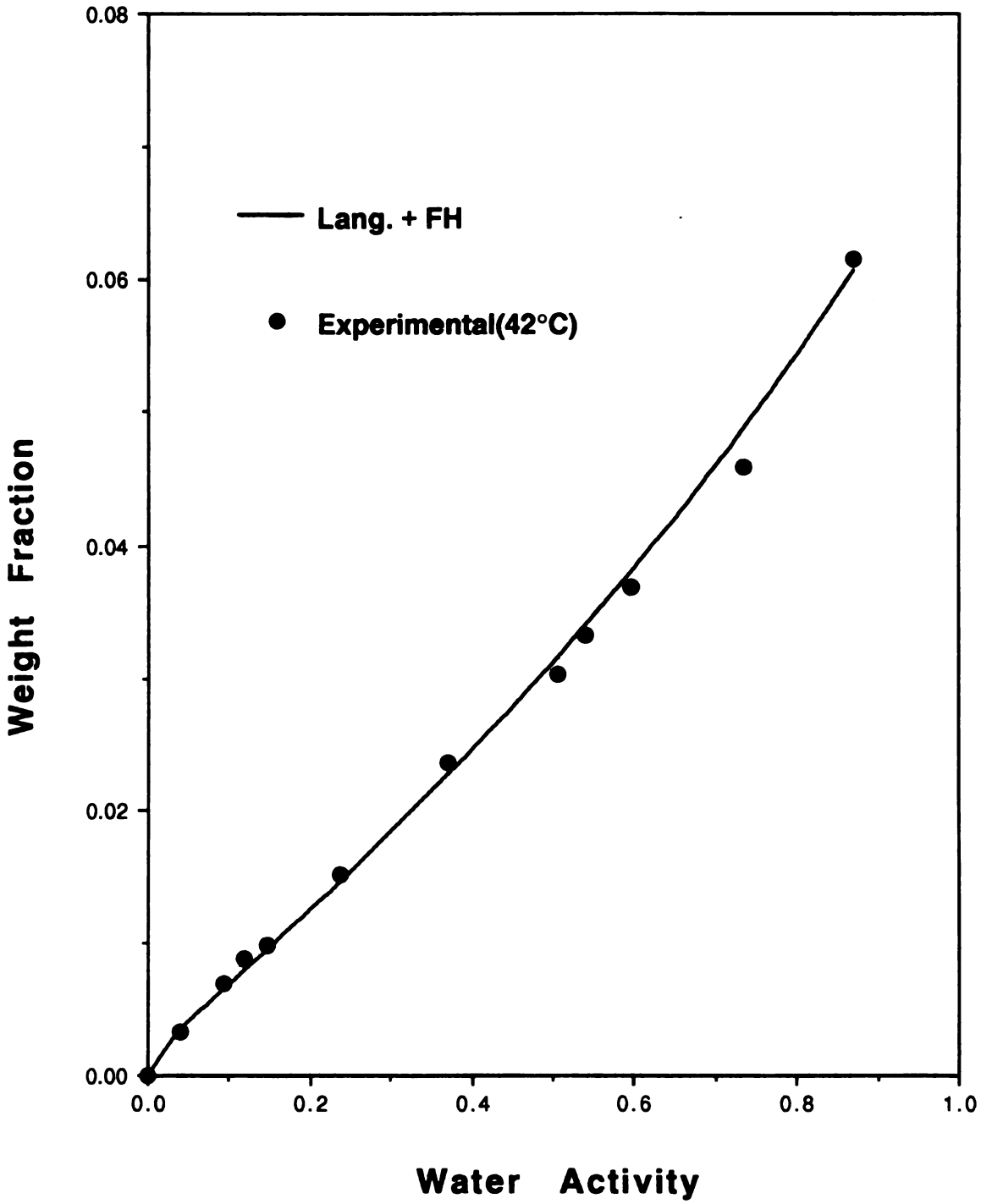

Figure 14. Best fit for the Langmuir-Flory-Huggins model

Values of parameters are CHI=1.99, K=0.147 and B=74.9

Table 5. Value of CHI, K and B as a function of temperature

	Temperature		
Parameter	5°C	23°C	42°C
CHI	1.782	1.913	1.993
K	0.1774	0.1518	0.1467
B	53.47	64.26	74.90

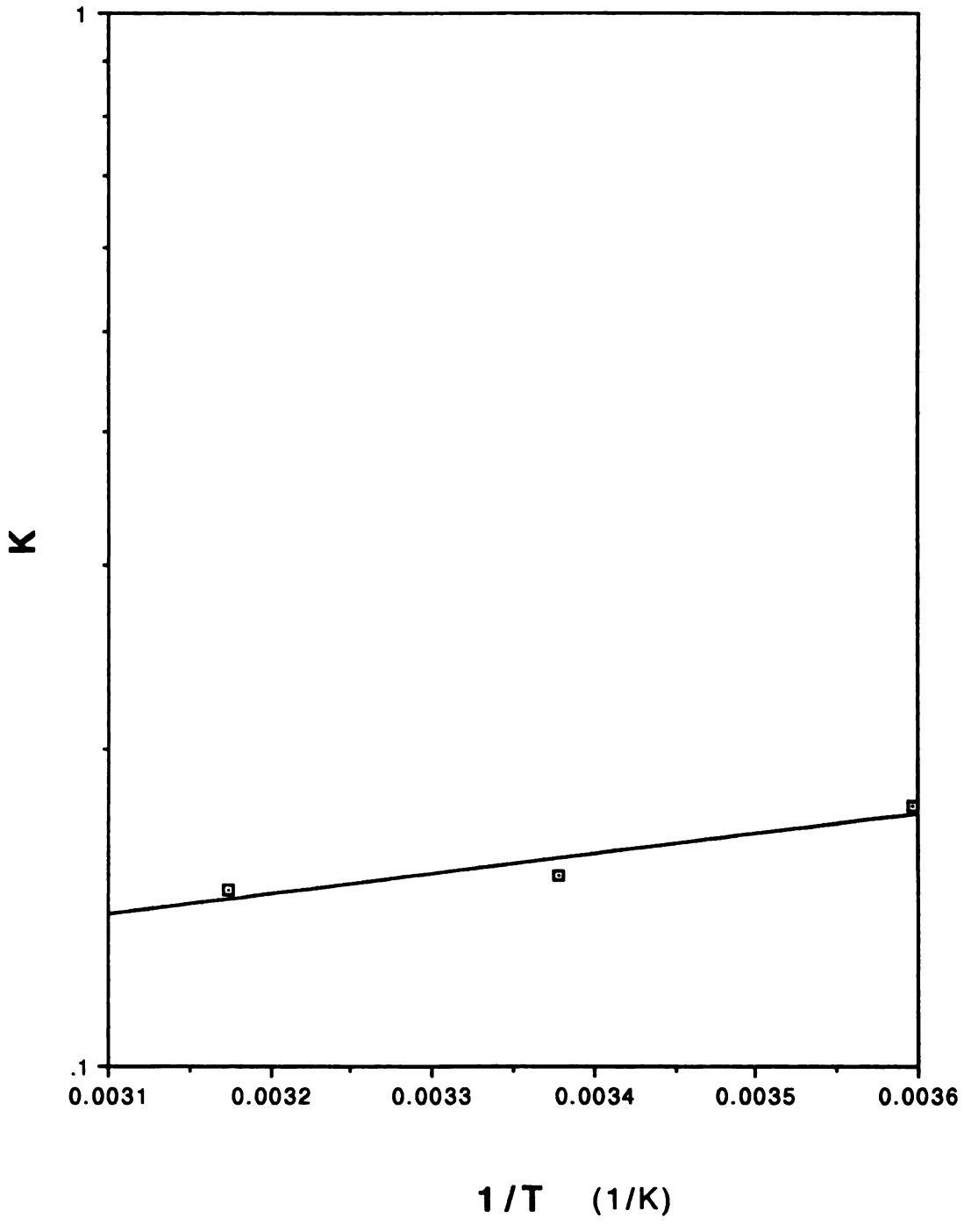

Figure 15. Arrhenius plot of K of the Langmuir equation

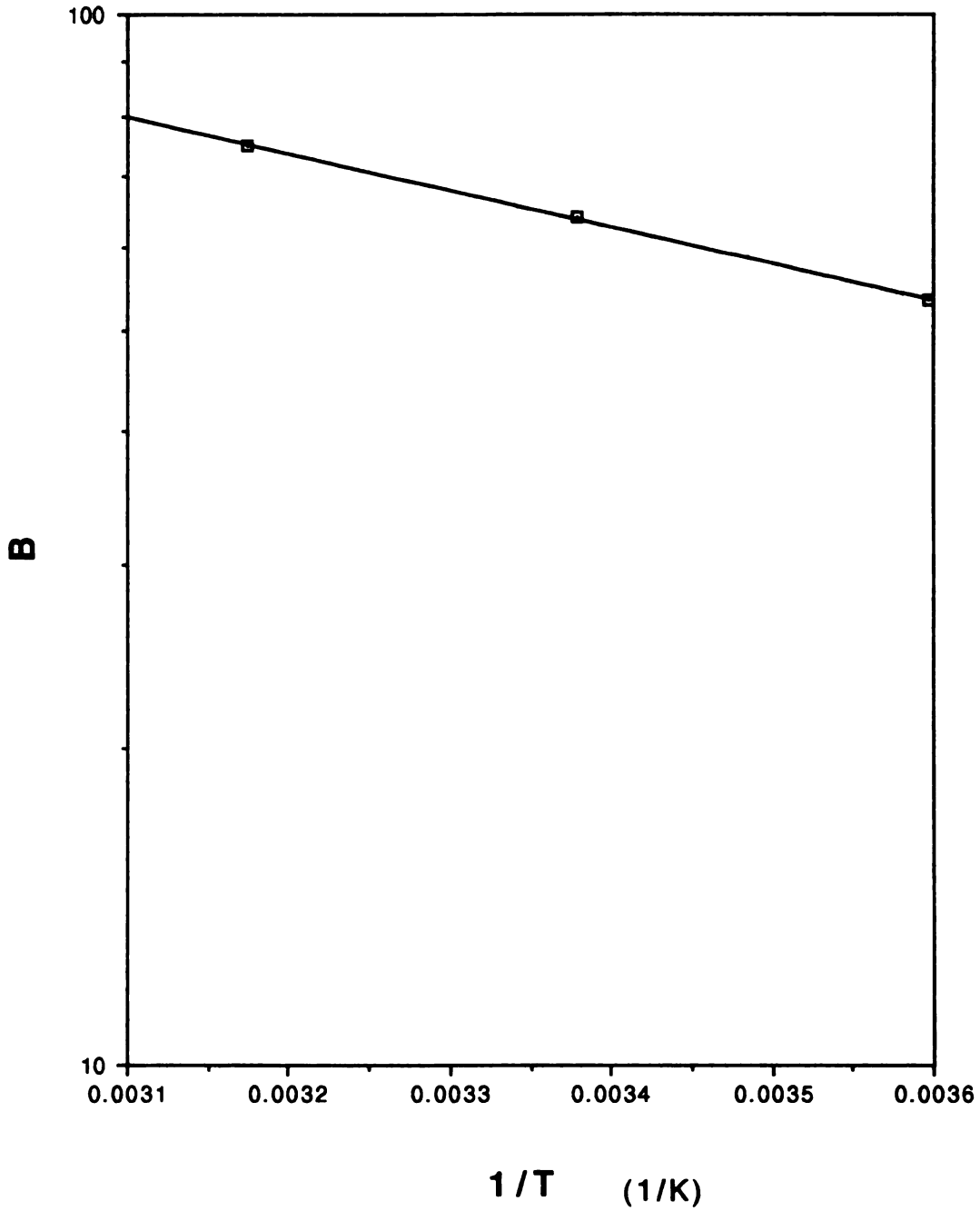

Figure 16. Arrhenius plot of B of the Langmuir equation

Table 6. Diffusion, solubility and permeability values of oxygen at 5°C

Water Activity	D x E09 (a)	S x10 (b)	P (c)
0	0.809	0.387	11.57
0.078	1.23	0.216	9.79
0.148	0.761	0.216	6.09
0.250	0.847	0.146	4.57
0.35	0.768	0.133	3.77
0.520	0.910	0.105	3.54
0.680	0.957	0.120	4.13
0.790	0.635	0.211	4.96
0.890	0.286	0.681	7.21

(a) - in (cm^2/sec)

(b) - in (cc O_2/cc polymer)

(c) - in (cc O_2 mil/m^2 day atm)

Table 7. Diffusion, solubility and permeability values of oxygen at room temperature

Water Activity	D x E09 (a)	S x10 (b)	P (c)
0	1.58	0.443	25.8
0.140	2.54	0.157	14.7
0.208	1.84	0.194	13.2
0.330	2.15	0.168	13.4
0.57	0.779	0.603	17.4
0.635	0.512	1.08	20.5
0.87	0.198	4.277	31.3
0.900	0.182	5.690	38.3

(a) - in (cm^2/sec)

(b) - in (cc O_2/cc polymer)

(c) - in (cc O_2 mil/m^2 day atm)

Table 8. Diffusion, solubility and permeability values of oxygen at 42°C

Water Activity	D x E09 (a)	S x10 (b)	P (c)
0	3.01	0.572	63.75
0.045	3.52	0.424	55.15
0.092	4.02	0.342	50.85
0.138	4.23	0.340	53.19
0.202	1.63	0.896	53.98
0.280	1.11	1.280	52.41
0.380	1.10	1.430	57.89
0.500	0.365	4.580	61.80
0.590	0.334	5.640	69.62
0.79	0.3101	9.420	104.48
0.890	0.293	11.60	125.20

(a) - in (cm^2/sec)

(b) - in (cc O_2/cc polymer)

(c) - in (cc O_2 mil/m^2 day atm)

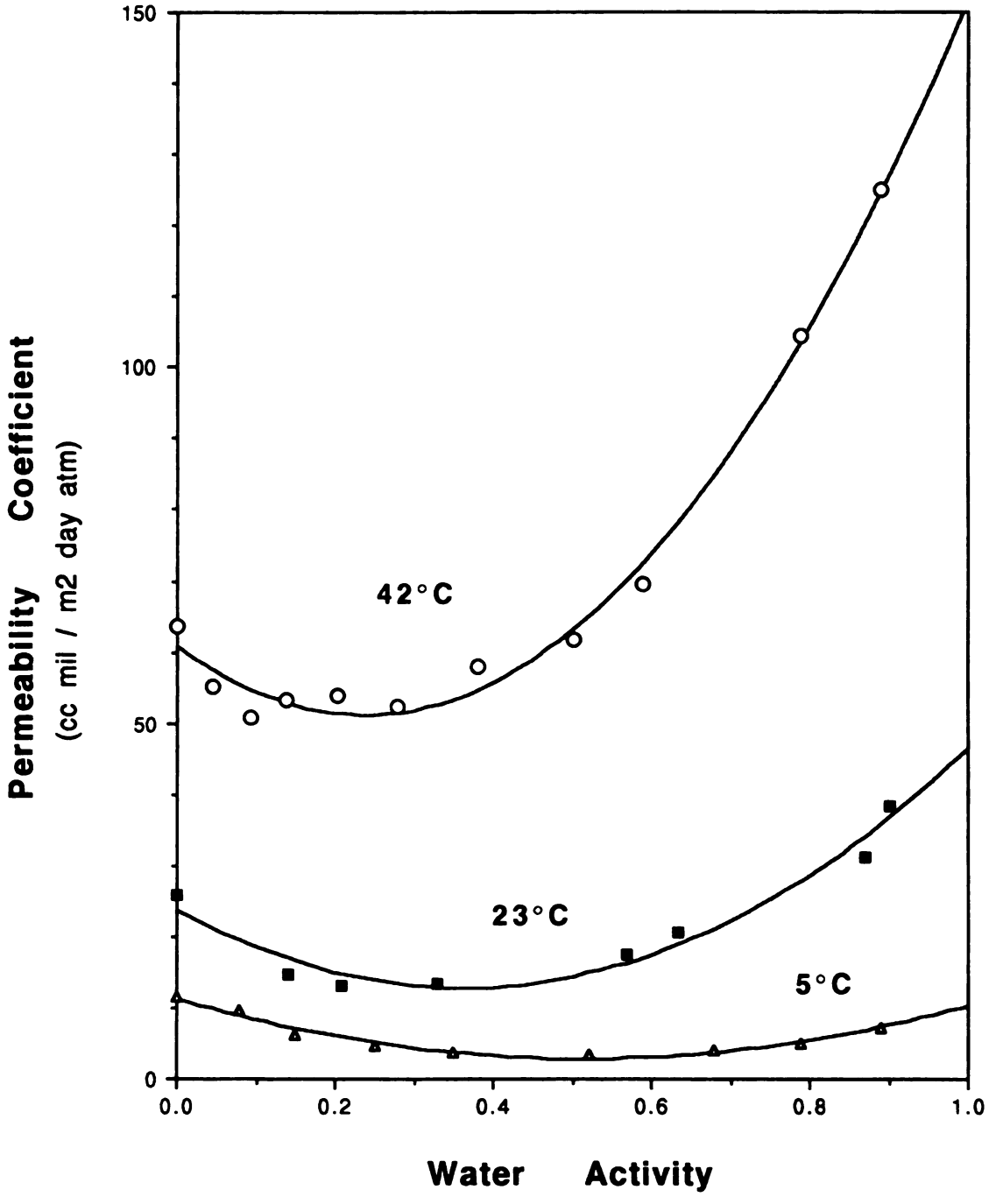

Figure 17. Oxygen permeability values at 5°C, 23°C and 42°C

(23°C) and 42°C, respectively. Figures 17 shows the effect of temperature on the permeability coefficient of oxygen in nylon-6, as a function of water activity. The diffusion coefficient and solubility values of oxygen in the polymer were also obtained from these experiments (Hernandez et al., 1986). The diffusion coefficient was calculated from a least-squares linear analysis of values from the unsteady state region for each permeability run. Solubility values were calculated from the eqn. (2). The solubility of oxygen (S) is expressed in cc O_2 (STP)/cc polymer-water system.

As shown in Figure 17, oxygen permeability decreased at the water activity levels below 0.3 and then increased at the high water activity, as a function of water activity. Generally, it has been proposed that oxygen permeability of nylon films, except amorphous nylon, increase as a function of water activity.

Figure 17, 18 and 19 illustrate the effect of temperature on the permeability coefficient, the diffusion coefficient and the solubility of oxygen in nylon-6, as a function of water activity respectively. The diffusion coefficients increase in the range of 0 to 0.2 water activity, and then decrease as further increase water activity. The observed increase of D in the region of low water activity may be attributed to a plasticization of amide chain backbone by sorbed water. This plasticization effect would tend to increase the mobility of oxygen molecules and polymer chain segments within the polymer bulk phase. Plasticization may also result in increase in the percent crystallinity (Clark and Wilson, 1973) (see following DSC experiments). Oxygen molecules cannot diffuse through the crystalline region, hence the diffusion coefficient tends to decrease in higher water activities. Above the water activity 0.5, the diffusion coefficient values at 23°C and 42°C were lower than those of 5°C. These

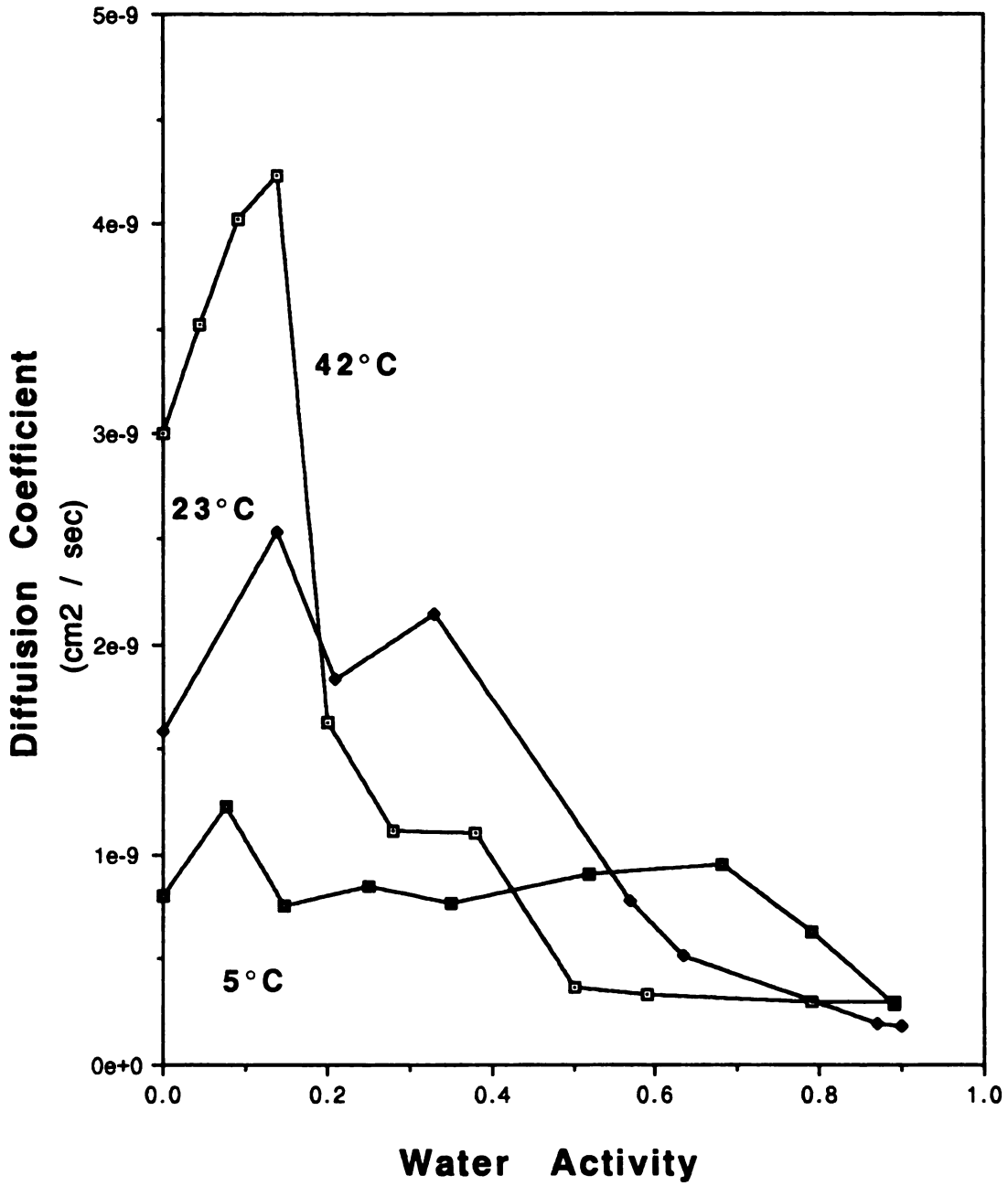

Figure 18. Diffusion coefficient values at 5°C, 23°C and 42°C

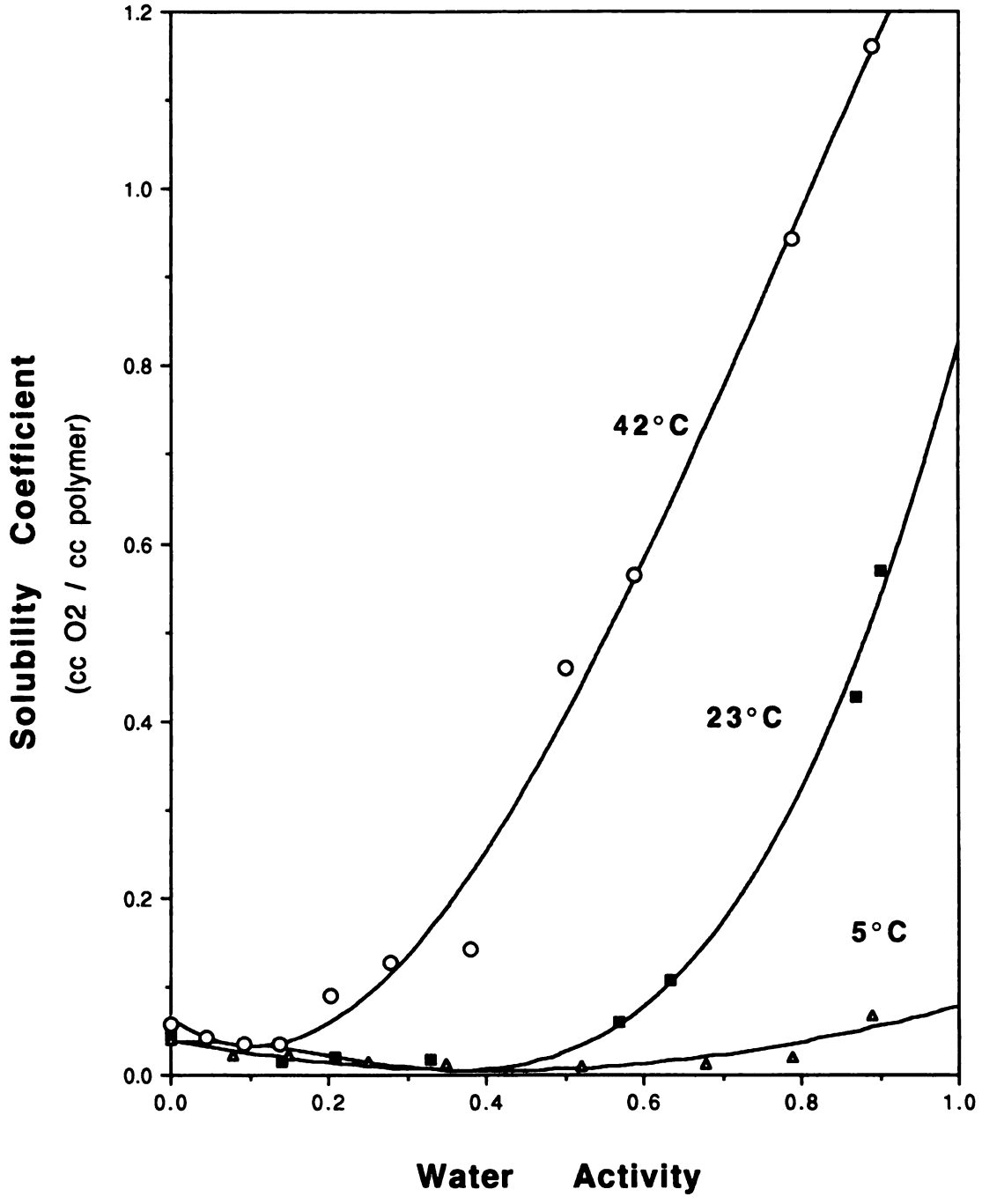

Figure 19. Solubility coefficient values at 5°C, 23°C and 42°C

results are not consistent, since the intersection of the curve should not happen. There must have been experimental errors such as the instrumental error of humidity sensers with this study. Therefore, further studies on the diffusion coefficient through a nylon-6 film should be conducted to confirm the results obtained in this study. However, the trend of values appears to be correct.

On the other hand, the solubility coefficients decrease in the range of low water activity, and then increase as a function of water activity. The high permeability coefficients of nylon-6 in the range of high water activity were attributed to the higher oxygen solubility coefficient values than the diffusion coefficient. The behavior of the solubility coefficient of nylon-6 is opposite, compared to that of nylon 6I/6T obtained by Hernandez et al. (1991). As mentioned above, the percent crystallinity of nylon-6 increases with water activity values. The crystallized molecules associated with water might be very small and disperse in the polymer. These small crystallized molecules might make the solubility coefficient increase with the water activity values. However, that is not fully understood. Further studies may be conducted to confirm this hypothesis.

Differential Scanning Calorimetry (DSC) Experiments

DSC method for determining the percent crystallinity of a nylon-6 film was used in this study. Table 9 shows the enthalpy data at the melting point and the percent crystallinity of nylon-6, as a function of water activity. Percent crystallinity values of the samples were calculated by using eqn. (1).

Table 9. The enthalpy at melting point and percent crystallinity for nylon-6 as a function of humidity

Conditions	Enthalpy at Melting Point (J/g) Replications 1	2	3	4	Enthalpy Mean	Percent Crystallinity Mean
Dry	64.3	61.6	61.9	59.0	61.7±2.17	31.7±1.11
33% RH	70.1	69.2			69.7±0.64	35.8±0.33
63% RH	72.4	65.9			69.2±4.60	35.5±2.36

Table 10. ANOVA for the DSC data (dry vs. 33% RH samples)

Source of Variation	Degree of Freedom df	Sum of Squares SS	Mean Square MS	Observed F	Required F	
					5%	1%
Total	5	98.3				
Varieties	1	83.8	83.8	23.1	6.94	18.00
Error	4	14.5	3.63			

Table 11. ANOVA for the DSC data (dry vs. 63% RH samples)

Source of Variation	Degree of Freedom df	Sum of Squares SS	Mean Square MS	Observed F	Required F	
					5%	1%
Total	5	109.2				
Varieties	1	74.0	74.0	8.41	6.94	18.00
Error	4	35.2	8.80			

Table 12. Student's t test of DSC data (dry vs. 33% RH samples)

Variable:	Dry	33% RH
Mean	61.70	69.65
Std.Deviation	2.168	0.636
Observations	4	2
t-test	-4.821	Hypothesis
Degree of Freedom	4	Ho: $\mu 1 = \mu 2$
Significance	0.009	Ha: $\mu 1 \neq \mu 2$

Table 13. Student's t test of DSC data (dry vs. 63% RH samples)

Variable:	Dry	63% RH
Mean	61.70	69.15
Std.Deviation	2.168	4.596
Observations	4	2
t-test	-2.899	Hypothesis
Degree of Freedom	4	Ho: $\mu 1 = \mu 2$
Significance	0.044	Ha: $\mu 1 \neq \mu 2$

The percent crystallinity of wet samples were higher than that of dry samples. Table 10 and 11 show the statistic analysis by ANOVA, and Table 12 and 13 show the results of the student t test. From these statistic results, there was a significant difference between percent crystallinity of dry nylon-6 and wet nylon-6 with 95 % confidence, in terms of the percent crystallinity of the dry and wet nylon-6 film.

The increase of percent crystallinity of nylon-6 might be the plasticization effect by water. Water is assumed to be distributed homogeneously throughout the polymer and it resides principally in the noncrystalline region. The water in amorphous region would cause the increase of percent crystallinity of nylon-6.

CONCLUSIONS

Sorption isotherm data of water vapor in nylon-6 film were obtained over a wide range water activities at 5°C, 23°C and 42°C. The modified dual sorption model which has been proposed by Hernandez et al. (1991) was found to describe well the sorption of water vapor by nylon-6 film. The dual mode sorption model is based on a Flory-Huggins and Langmuir equation and was developed to describe water vapor sorbed by an amorphous polyamide. Hernandez et al. used a nonlinear regression method to determine the values of three parameters of the Langmuir Flory-Huggins equation. In this study, a computer program was developed and it was useful to determine the three parameters.

The oxygen permeability behavior was analyzed in terms of the multiplicative effect of a mobility and solubility term. The oxygen permeability coefficient for nylon-6 decreased in the range of 0 to 0.3 water activities, and then increased at the high water activities. This result was different from general belief in which oxygen permeability of semicrystalline nylon increases continually as a function of moisture content of the polymer. The oxygen diffusion coefficient values appears to decrease above 0.2 of water activity and the solubility of oxygen showed a steadily increase at the high water activity. The combination of these two effects resulted in the observed increase of the oxygen permeability values above 0.3 of water activity as a function of water content in nylon-6.

There was a statistically significant increase of crystallinity of wet

nylon-6 film compared to the dry sample. The percent crystallinity of samples with a water activity above 0.3 were higher than that of dry. The change in morphology may be associated with the decrease of the oxygen diffusion coefficients as well as the increase of the oxygen solubility in the water / nylon-6 system.

APPENDIX

APPENDIX A

Computer Program For Flory-Huggins Model

```
100 REM BOX KANAMAZU METHOD FOR FLORY HUGGINS MODEL
105 REM PROGRAM WRTTEN BY DR. R.J. HERANADEZ, 1988
110  CLS:  DIM  A1(20),V1(20),ETA(20),X(20)
120 INPUT  "HOW MANY POINTS?",  N
130 INPUT "HOW MANY ITERATIONS?",  ITE
140 INPUT "ENTER THE FIRST ESTIMATE OF CHI",  B
150 PRINT "ENTER FIRST A1'S AND THEN V1'S"
160   A1(1)=.069:A1(2)=.13:A1(3)=.182:A1(4)=.26:A1(5)=.37:A1(6)=.44
170   A1(7)=.65:A1(8)=.95
190   V1(1)=.00683:V1(2)=.012:V1(3)=.01447:V1(4)=.0202
200   V1(5)=.0289:V1(6)=.035:V1(7)=.0533:V1(8)=.0893
210 PRINT "      H", "SO",  "    S1", "   CHI"
220  RL=0!
225  RL=RL+1
230 XTX=0! : XTY=0! :SO=0! :S1=0!
240 REM EQUATION FOR THE MODEL
250 FOR K=1 TO N
255   V2=1-V1(K)
260   ETA(K)=V1(K)*EXP(V2+B*V2*V2)
270 NEXT K
280 REM EQUATION FOR THE SENSITIVITY COEFF
290 FOR K=1 TO N
295   V2=1!-V1(K)
300   X(K)=V1(K)*V2*V2*EXP(V2+B*V2*V2)
310 NEXT K
315 REM CALCULATE 2O,  XTX,  XTY
320 FOR K=1 TO N
330   SO=SO+(A1(K)-ETA(K))*(A1(K)-ETA(K))
340 XTX=XTX+X(K)*X(K)
350  XTY=XTY+X(K)*(A1(K)-ETA(K))
360 NEXT K
370 DELTAB=XTY/XTX
380 REM CALCULATE G
390  G=DELTAB*DELTAB*XTX
400 IF (G<0!) OR (G=0!) GOTO 670
410  H=1!
```

```
420 B=B+DELTAB*H
430 REM CALCULATE ETA'S WITH B'S
440 FOR K=1 TO N
445  V2=1!-V1(K)
450  ETA(K)=V1(K)*EXP(V2+B*V2*V2)
460 NEXT K
560 REM CALCULATE S1
570 FOR K=1 TO N
580  S1=S1+(A1(K)-ETA(K))*(A1(K)-ETA(K))
590 NEXT K
600  JJ=SO-(2-(1/1.1))*G
610 IF (S1<JJ) OR (S1=JJ) GOTO 640
615 B=B-DELTAB*H
620 H=G/(S1-SO+2!*G)
630 B=B+H*DELTAB
640 PRINT H,SO,S1,B
650 IF (RL<ITE+1) GOTO 225
660 IF (RL=ITE) GOTO 680
670 PRINT "G=",G
680 END
```

APPENDIX B

Computer Program For Langmuir-Flory-Huggins Model

```
100 REM THIS PROGRAM CALCULATES K AND B FOR LANGMUIR
102 REM COMPONENT FRACTION GIVEN CHI THAT HAS BEING OBTAINED
104 REM USING FLORY.BAS IT TAKES THE DIFFERENCE BETWEEN
      EXPERIMENT SORPTION VALUES
106 REM AND DO A LEAST SQUARE ANALYSIS TO GET K AND B
108 REM IT ALSO GIVES THE CORRELATION COEFFICIENT FOR
110 REM THE LINEAR CORRELATION AS WELL AS THE SUM OF SQUARE
112 REM FOR THE EXPERIMENTAL AND LANGMUIR-FLORY-HUGGINS
      MODEL
118  DIM  A(30),  W(30),M(30),L(30),LG(30),MFH(30)
121   A(1)=0l:A(2)=.067:A(3)=.096:A(4)=.148:A(5)=.182:A(6)=.238
122   A(7)=.306:A(8)=.38:A(9)=.47:A(10)=.52:A(11)=.55
125   A(12)=.65:A(13)=.79
126   M(1)=0l:M(2)=.0055:M(3)=.0074:M(4)=.0108:M(5)=.0126
127   M(6)=.0162:M(7)=.0206:M(8)=.0257:M(9)=.0312
128   M(10)=.035:M(11)=.0376:M(12)=.0454:M(13)=.0587
135 INPUT "ENTER VALUE OF CHI    ",CHI
140 LPRINT "CHI VALUE USED=";CHI
145 LPRINT "ACTIVITY";  "      EXPERIMENT";  "          F-H";   "
      LANG."  "              MFH"
150 FOR I=1 TO 13
155 REM FIRST GUESS FOR VOLUME FRACTION : X=A(I)/10
160 FOR II=1 TO 4
170  Z=1-X
180  Y=Z+CHI*Z*Z
190  F=X*EXP(Y)-A(I)
200   FP=EXP(Y)*(1-X*(2*CHI*Z+1))
210  X=X-F/FP
215  W(I)=X
220 NEXT II
224 REM CALCULATE EXPERIMENT F-H TO GIVE LANG.  COMP.
230 SA=0:  SSA=0:  SL=O:SAL=0:SSL=0
240 NEXT I
243 FOR I=2 TO 13
250 REM LINEAR REG.  TO CALCULATE K&B IN LAPY
255   L(I)=M(I)-W(I)
```

```
260  SL=SL+(1/L(I))
270  SA=SA+(1/A(I))
280  SAL=SAL+(1/A(I))*(1/L(I))
290  SSA=SSA+(1/A(I))*(1/A(I))
295  SSL=SSL+(1/L(I))*(1/L(I))
300 NEXT I
302 PRINT "SL="SL,  "SA="SA,
303 PRINT "SAL="SAL,  "SSA="SSA
310 REM CALCULATE K
315  K=(12*SSA-SA*SA)/(12*SAL-SA*SL)
320 REM CALCULATE B/K
325  BOK=((SL*SSA)-(SA*SAL))/((12*SSA)-SA*SA)
330 B=BOK*K
340 REM CALCULATE SUM OF SQUARE FOR EXPERIMENTAL AND
      CALCULATED,SST
345 SST=0
350 FOR I=1 TO 13
370  LG(I)=K*A(I)/(1+B*A(I))
380 SST=SST+((M(I)-W(I))-LG(I))^2
400 MFH(I)=W(I)+LG(I)
430 LPRINT  A(I);   M(I);    W(I);   LG(I);      MFH(I)
440 NEXT I
450 SY=0:SAY=0
455 FOR I=2 TO 13
460  SY=SY+(1/L(I)-BOK-(1/K)*(1/A(I)))^2
465  SAY=SAY+(1/L(I)-SL/12)^2
468 NEXT I
470 REM CALCULATE CORRELATION COEFFICIENT
475 SR=1-SY/SAY
480 LPRINT "SUM OF SQUARE ="SST,  "K="K,  "B="B,  "SR="SR
490 END
```

APPENDIX C

Computer Program For Diffusion And Solubility Coeff.

```
100 REM THIS PROGRAM CALCULATES THE DIFFUSION COEFFICIENT
      FROM PERMEABILITY
102 REM CONTINUOUS FLOW EXPERIMENTS
104 REM PROGRAM WRITTEN NY R. J. HERNANDEZ. JAN/1988.
      MODIFIED FOR K. OHASHI
106 REM ON 11-7-'90
110 DIM F(50),T(50),X(50),DF(50)
120 REM THE UNITS OF TIME USED WILL DETERMINE THE UNITS IN THE
      DIFF.COEFF
132 PRINT "ENTER RELATIVE HUMIDITY IN PERCENT"
133 INPUT HUM
135 PRINT "ENTER THE RUN IDENTIFICATION NUMBER"
136 REM
137 INPUT SUN
138 PRINT "ENTER THE TEMPERATURE AT STEADY STATE"
139 INPUT W
140 PRINT "ENTER THE NUMBER OF DATA POINTS"
150 INPUT D
160 PRINT "ENTER THE FLOW F AND TIME T STARTING FRO ZERO"
170 FOR I=1 TO D
180 PRINT "ENTER F"
190 INPUT F(I)
200 PRINT "ENTER T"
210 INPUT T(I)
220 NEXT I
230 PRINT "ENTER YOUR GUESS FOR X"
270 INPUT GUESS
280 PRINT "ENTER INFINITE VALUE FOR X"
270 INPUT FI
300 FOR I=1 TO D
305 DF(I)=F(I)/FI
310 A=.44313*F(I)/FI
320 X=GUESS
330 FOR J=1 TO 7
340 B=SQR(X)
350 C=EXP(-X)
```

```
360  L=1/B
370  H=(.5*L-B)*C
380  E=(B*C)-A
390  X=X-(E/H)
400 NEXT J
410  X(I)=X
420 GUESS=X
430 NEXT I
480 REM LINEAR REGRESSION
490  ST=0
500  SX=0
510  SXT=0
520  STSQ=0
530 SXSQ=0
540 FOR I=1 TO D
545  X(I)=1!/X(I)
550  ST=ST+T(I)
560  SX=SX+X(I)
570  SXT=SXT+(X(I)*T(I))
580  SXSQ=SXSQ+(X(I)*X(I))
590  STSQ=STSQ+(T(I)*T(I))
600 NEXT I
610  SLOPE=(ST*SX-D*SXT)/(ST*ST-D*STSQ)
620  DUM1=(D*SXT)-(SX*ST)
630  DUM2=(D*STSQ)-(ST*ST)
640  DUM3=(D*SXSQ)-(SX*SX)
650 DUM4=SQQR(DUM2*DUM3)
660 R=DUM1/DUM4
662 LPRINT "RUN NUMBER:' SUN
663 PRINT
664 LPRINT "TIME (MIN)  ","FLOW",  "X",  "FLOW PERCENT"
670 FOR I=1 TO D
700  LPRINT  T(I),F(I),X(I),DF(I)
720 NEXT I
730 PRINT
735  DIFF=(4.2E-08)*SLOPE
736 LPRINT "DIFFSION COEFF IN cm2/sec. =" DIFF
737 LPRINT
738 LPRINT "THE PERMEABILITY COEFF IN cm3.mil/m2.day.atm ="
      FI*6.258*1.25
739 LPRINT
740 LPRINT "THE SLUBILITY IN  cc O2/cc olymer   ="
      (.0000000000211497#)*FI/DIFF
```

```
742 LPRINT
745 LPRINT "THE CORRELATION COEFF. =" R
746 LPRINT
747 LPRINT "TEMPERATURE IN C =" W
748 LPRINT "WATER ACTIVITY aw =" HUM/100
750 REM THE VALUE OF THE DIFFUSION COEFFICIENT IS FOR THE TIME
      IN MINUTES
755 REM THE THICKNESS IS L=3.175E-03 cm (1.250 mil)
800 END
```

APPENDIX D

Differential Scanning Calorimetry (DSC) Data

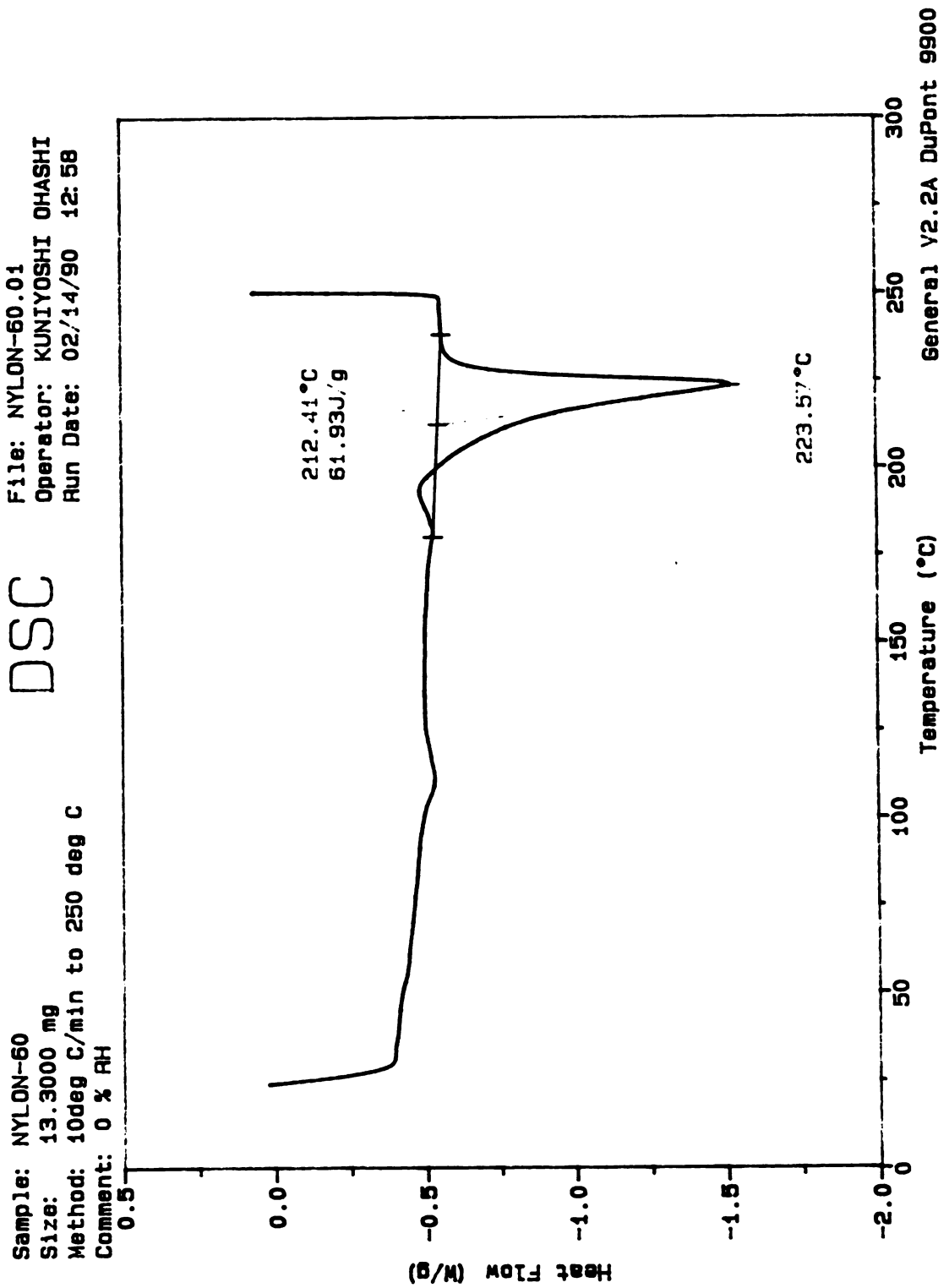
Sample: NYLON-60
Size: 13.3000 mg
Method: 10deg C/min to 250 deg C
Comment: 0 % RH
DSC
File: NYLON-60.01
Operator: KUNIYOSHI OHASHI
Run Date: 02/14/90 12:58
212.41°C
61.93J/g
223.57°C
Heat Flow (W/g)
Temperature (°C)
General V2.2A DuPont 9900

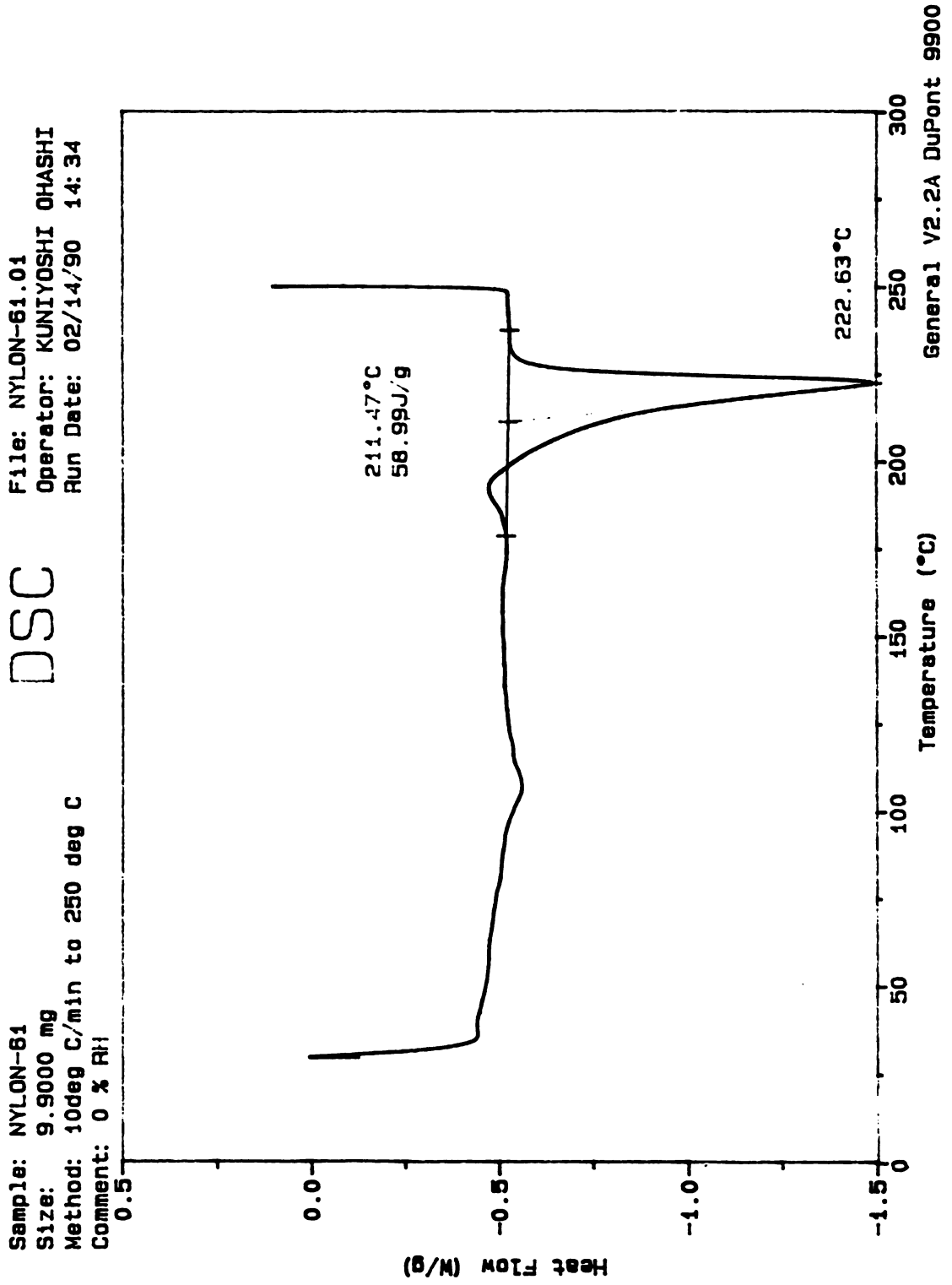
Sample: NYLON-61
Size: 9.9000 mg
Method: 10deg C/min to 250 deg C
Comment: 0 % RH
DSC
File: NYLON-61.01
Operator: KUNIYOSHI OHASHI
Run Date: 02/14/90 14:34
211.47°C
58.99J/g
222.63°C
Heat Flow (W/g)
Temperature (°C)
General V2.2A DuPont 9900

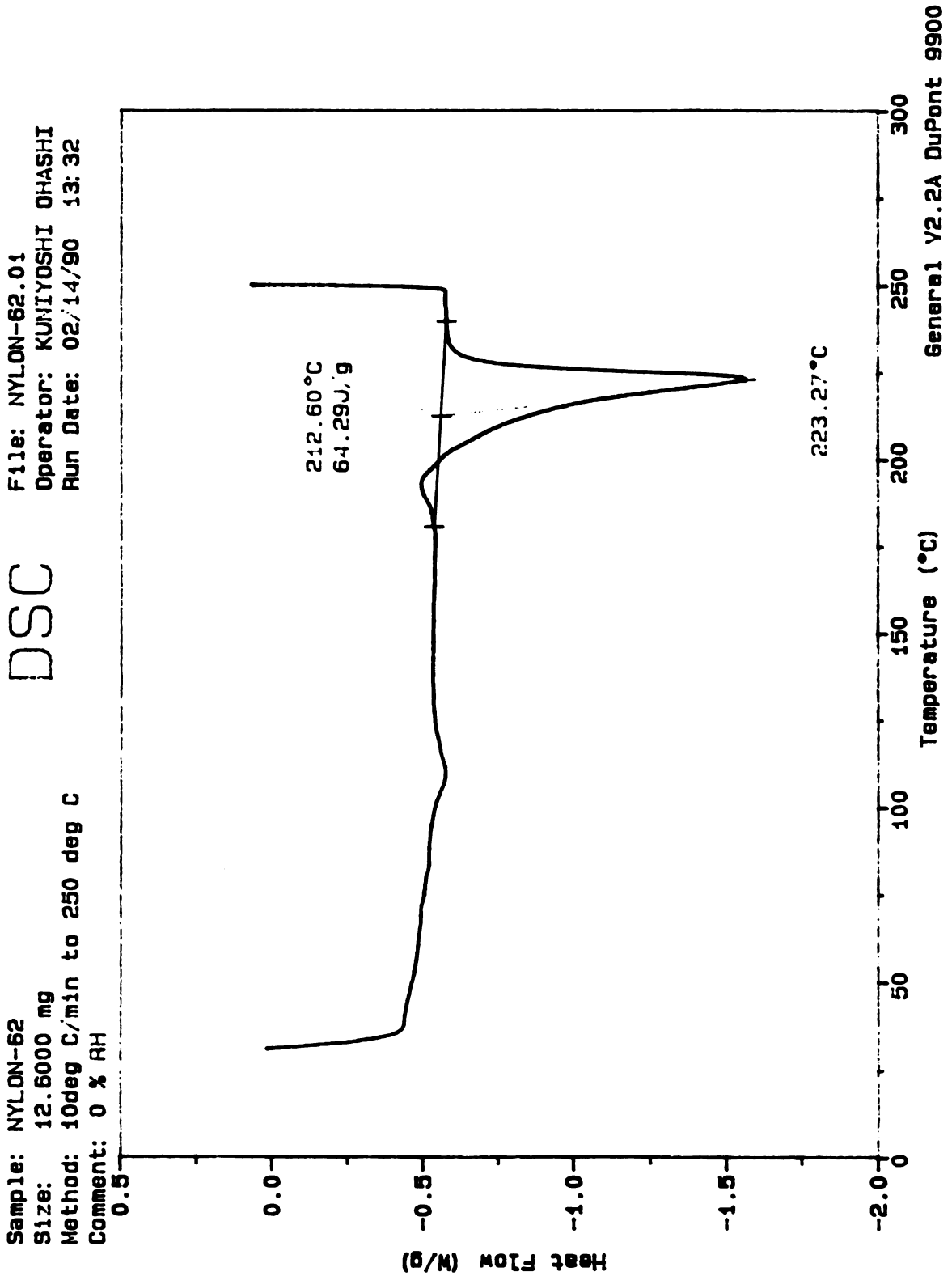
Sample: NYLON-62
Size: 12.6000 mg
Method: 10deg C/min to 250 deg C
Comment: 0 % RH
DSC
File: NYLON-62.01
Operator: KUNIYOSHI OHASHI
Run Date: 02/14/90 13:32
212.60°C
64.29J/g
223.27°C
Heat Flow (W/g)
0.5
0.0
-0.5
-1.0
-1.5
-2.0
0
50
100
150
200
250
300
Temperature (°C)
General V2.2A DuPont 9900

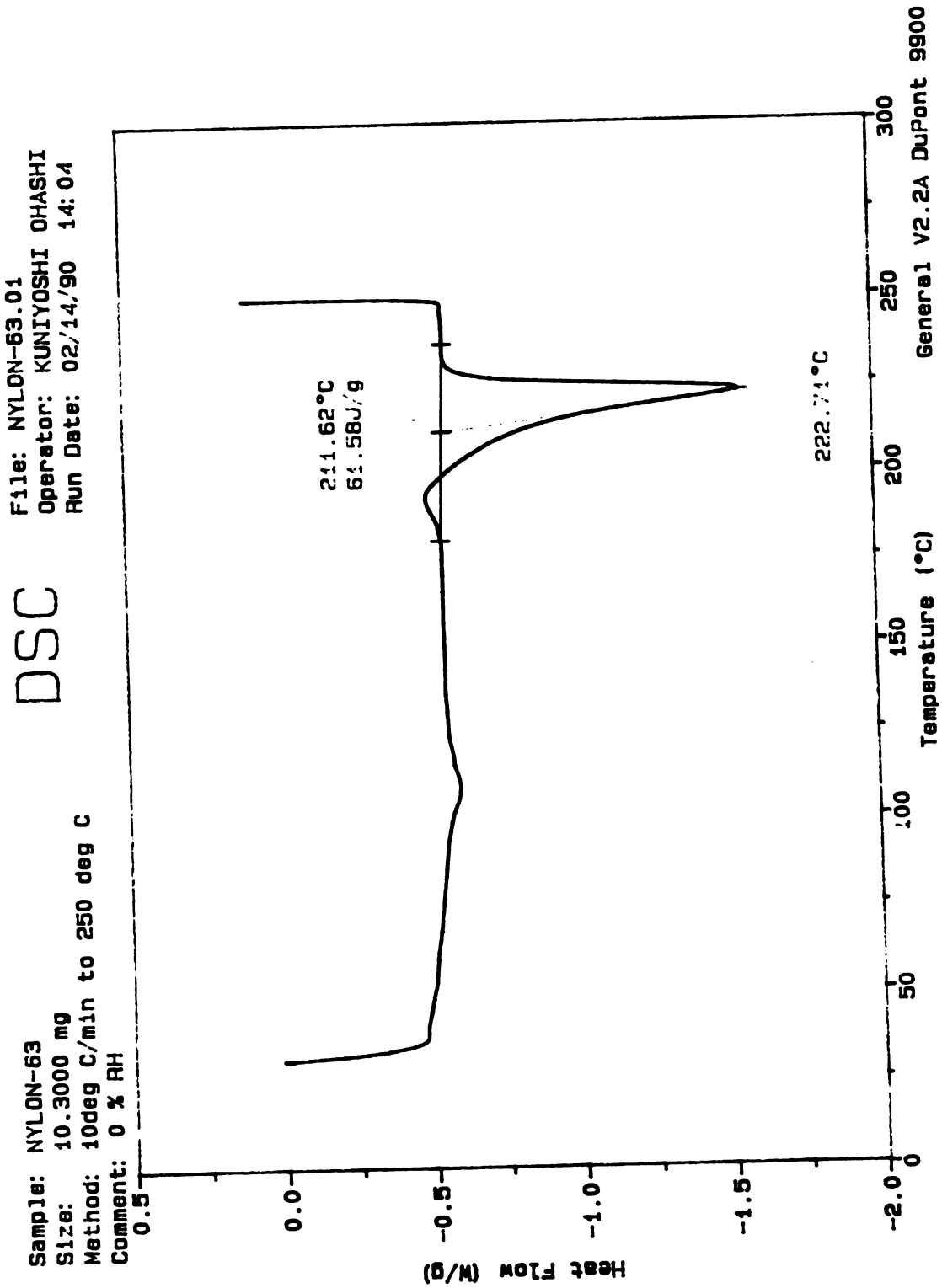
DSC
File: NYLON-63.01
Operator: KUNIYOSHI OHASHI
Run Date: 02/14/90 14:04
Sample: NYLON-63
Size: 10.3000 mg
Method: 10deg C/min to 250 deg C
Comment: 0 % RH
211.62°C
61.58J/g
222.71°C
Heat Flow (W/g)
Temperature (°C)
General V2.2A DuPont 9900

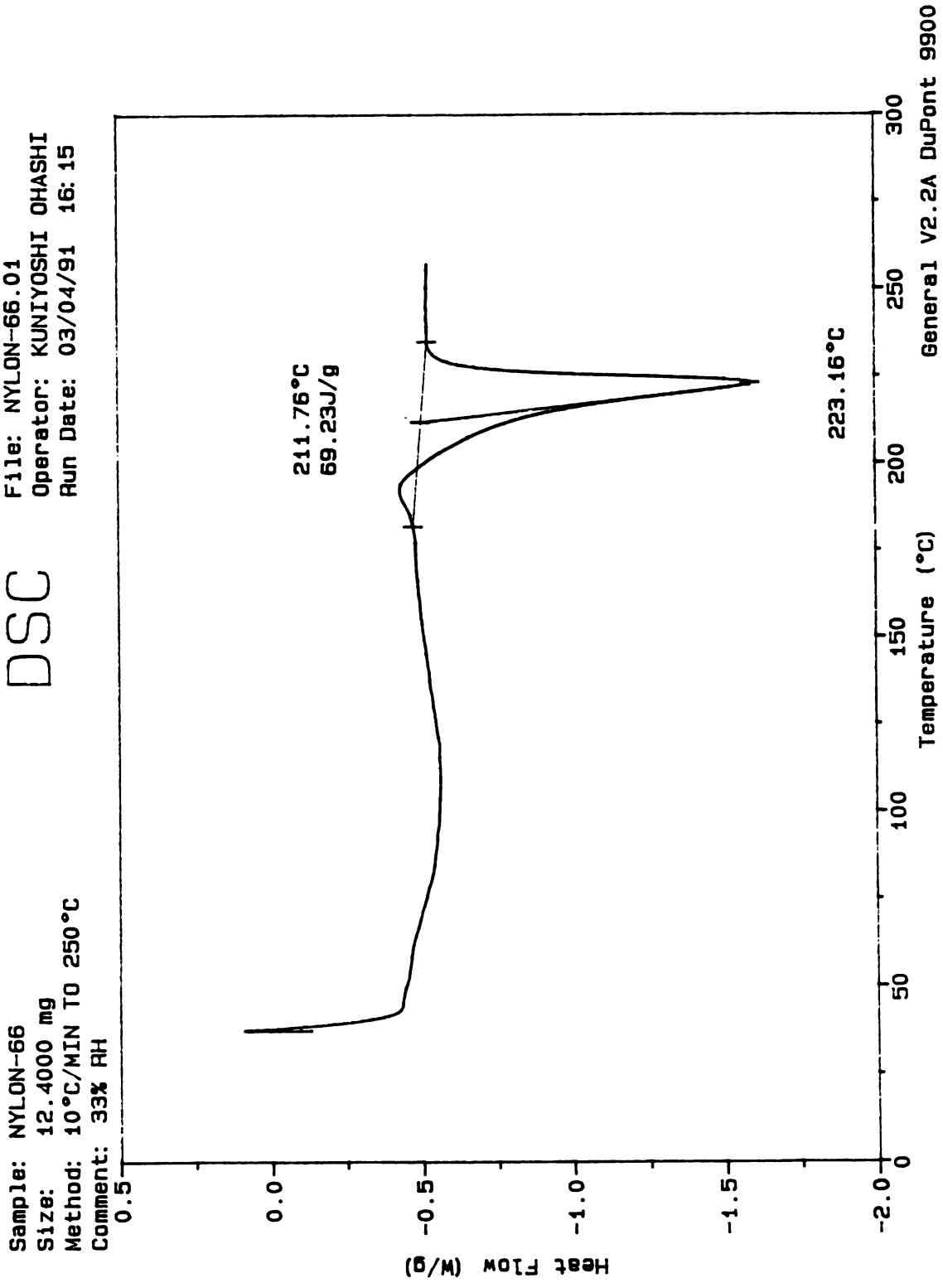
Sample: NYLON-66
Size: 12.4000 mg
Method: 10°C/MIN TO 250°C
Comment: 33% RH
DSC
File: NYLON-66.01
Operator: KUNIYOSHI OHASHI
Run Date: 03/04/91 16:15
211.76°C
69.23J/g
223.16°C
Heat Flow (W/g)
Temperature (°C)
General V2.2A DuPont 9900

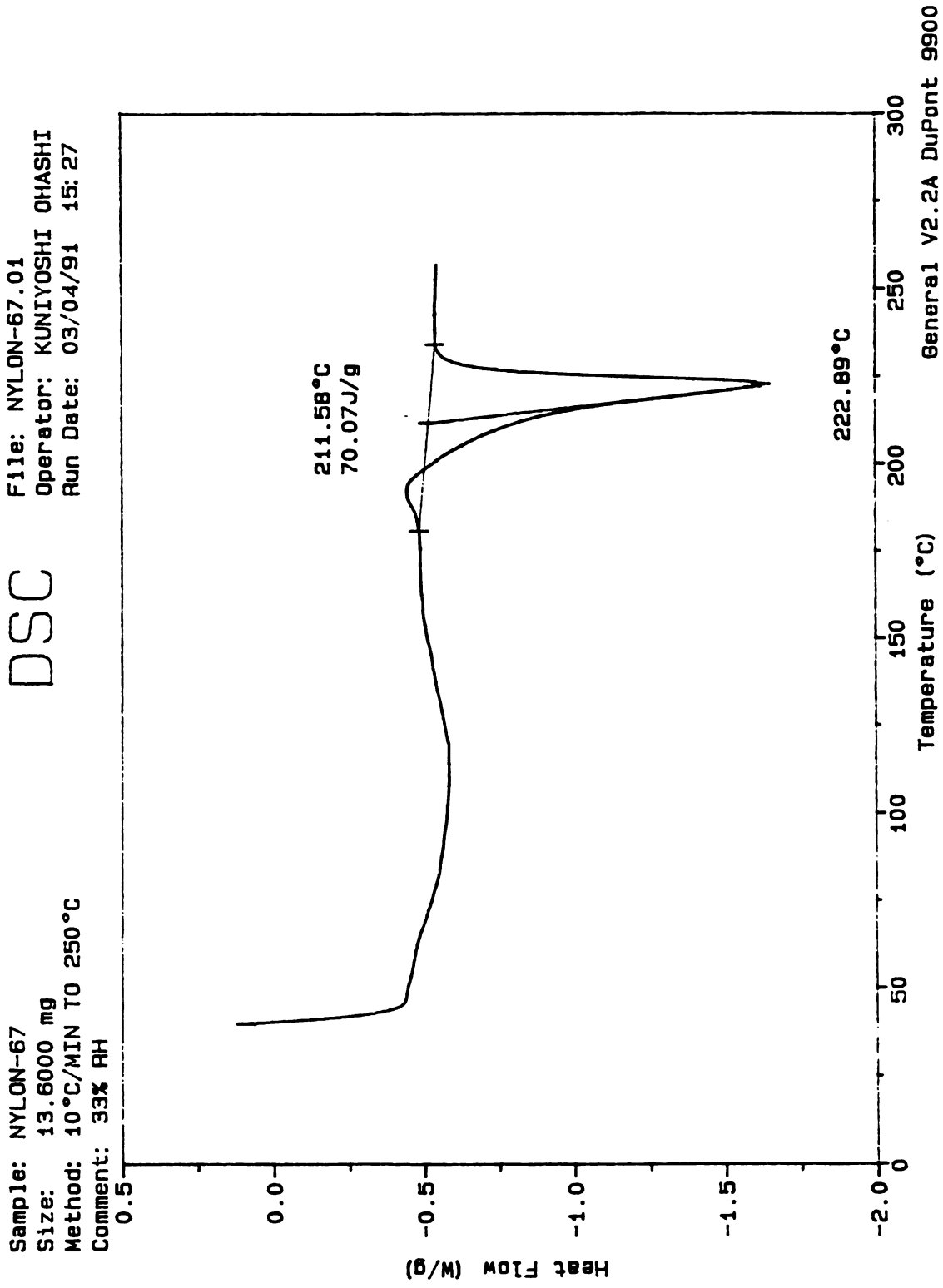
Sample: NYLON-67
Size: 13.6000 mg
Method: 10°C/MIN TO 250°C
Comment: 33% RH
DSC
File: NYLON-67.01
Operator: KUNIYOSHI OHASHI
Run Date: 03/04/91 15:27
211.58°C
70.07J/g
222.89°C
Heat Flow (W/g)
Temperature (°C)
General V2.2A DuPont 9900

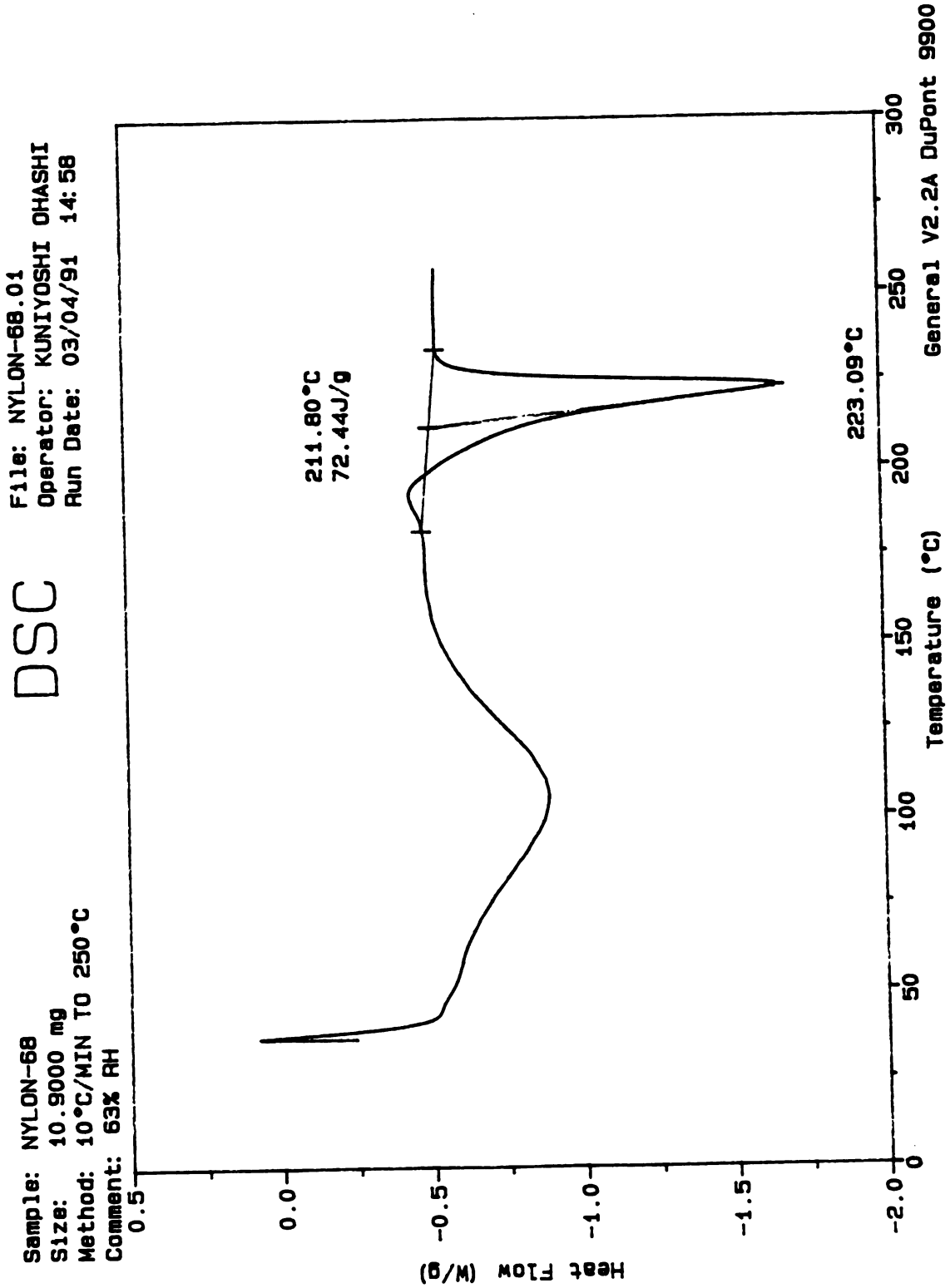
DSC
File: NYLON-68.01
Operator: KUNIYOSHI OHASHI
Run Date: 03/04/91 14:58
Sample: NYLON-68
Size: 10.9000 mg
Method: 10°C/MIN TO 250°C
Comment: 63% RH
211.80°C
72.44J/g
223.09°C
Heat Flow (W/g)
Temperature (°C)
General V2.2A DuPont 9900

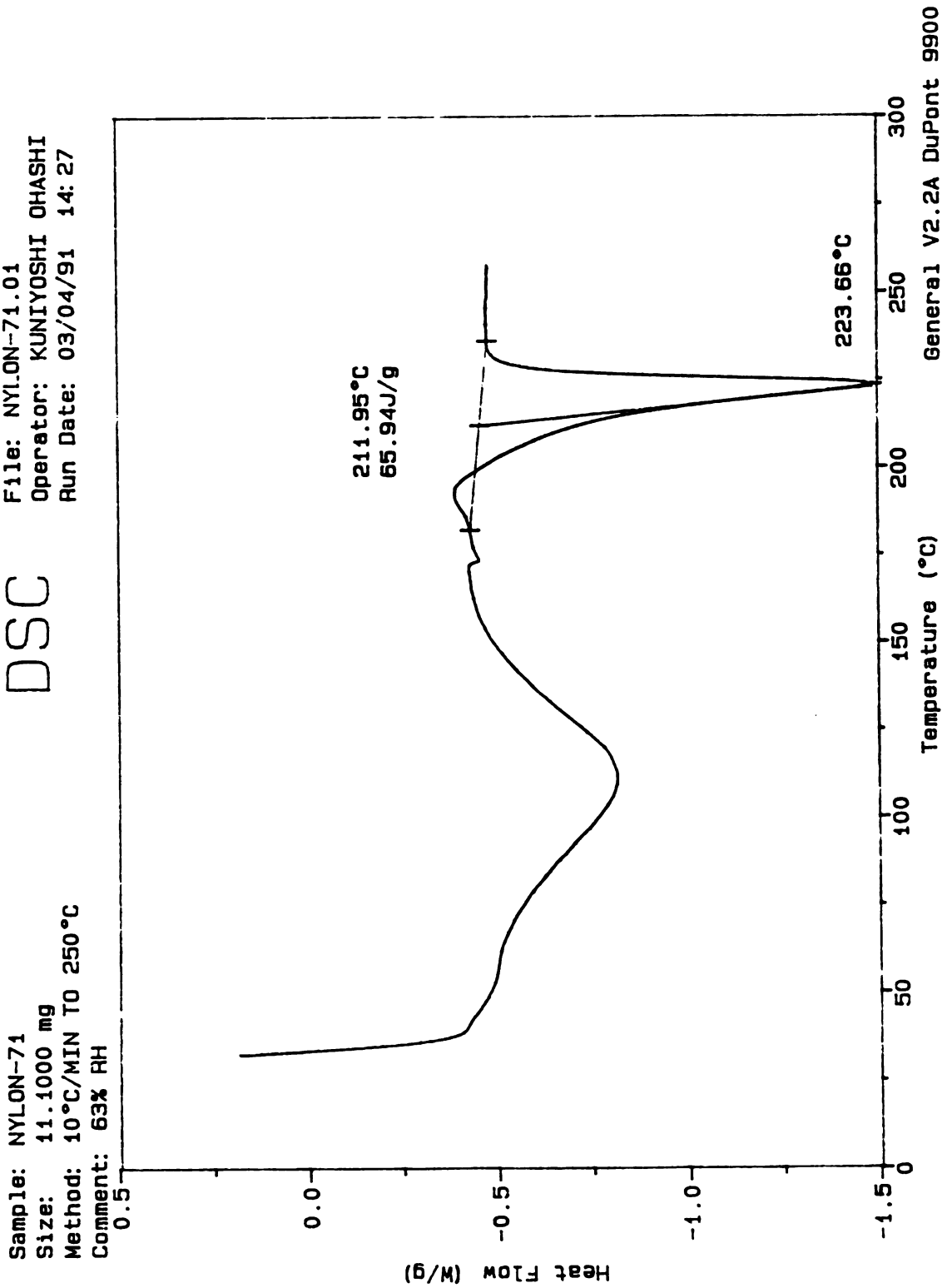
Sample: NYLON-71
Size: 11.1000 mg
Method: 10°C/MIN TO 250°C
Comment: 63% RH
DSC
File: NYLON-71.01
Operator: KUNIYOSHI OHASHI
Run Date: 03/04/91 14:27
211.95°C
65.94J/g
223.66°C
Heat Flow (W/g)
Temperature (°C)
General V2.2A DuPont 9900

BIBLIOGRAPHY

BIBLIOGRAPHY

Banks, L. and Ellis, B., 1979. Polym. Bull., 1, 377.

Barres, R., Barrier, J. and Slater, J., 1957. J. Polym. Sci., 23, 315.

Barrie, J. A., P. S. Sagoo and P. Johncock, 1984. J. Membrane Sci., The Sorption and Diffusion of Water in Epoxy Resins, 18, 197.

Beatty, C. L. and Karasz, F. E., 1975. Am. Chem. Soc. Div. Org. Coat. Plast. Prepr., 31, 370.

Berens, A. R., 1975. Anrew. Makromol. Chem., 47, 97.

Berens, A. R., 1985. "J. American Water Works Assoc., Nov., 57.

Blatz, Philip S., 1989. "Innovations in polyamide technology" AICHE meeting.

Bonner, R. M. , M. I. Kohan, E. M. Lacey, P. N. Richrdson, T. M. Roder, and L T. Sherwood, Jr. 1973. "Nylon Plastics" pp 365. John Wiley & Sons, N. Y.

Boyer (ed), 1977. "Encyclopedia of Polymer Science and Technology, Supplement no. 2". J. Wiley & Sons, N.Y.

Boyer, R. F., 1977. J. Appl. Phys., 20, 540.

Bradrup, J., and Immergut, E. H, Ed. 1991. Polymer Hand Book, interscience, New York.

Brunauer, S., Emmett, P. H., and E. Teller, 1938. J. Am. Chem. Soc., 60, 309.

Cambell, G. A., 1969. J. Polymer Science, 7B, 629.

Clark, E. S. and Wilson, F. C., 1973. "Nylon Plastics" John Wiley & Sons, N. Y.

Crank, J. and Park, 1968. "Diffusion In Polymers". Academic Press, N.Y.

Ellis, T. S. and Karasz, F. E., 1984. Polymer, 25, 664.

Fujita, H., 1961. Diffusion In Polymer-Diffuent Systems. Fortschr. Hochpolym. Forsh. 3(9), 1.

Fuzek, J. F., 1980. "Water in polymers" Am. Chem. Soc. Symp. Ser. 127, S. P. Rowland, Ed., American Chemical Society, Washington, DC.

Hernandez, R. J., J. R. Giacin and A. L. Baner, 1986. The Evaluation of the Aroma Barrier Properties of Polymer Films, J. Plastic film Sheeting, 2, 187-211.

Hernandez, R. J., J. R. Giacin and E. A. Gruke, (1991). "The Sorption of Water Vapor by an Amorphous Polyamide", J. Membr. Sci. (in press)

Hopfenberg, H. B., and Stannet, V., 1973. "The Physics of Glassy Polymers", R. N. Haward (ed), ch. 9, The diffusion and Sorption of Gases and Vapors in Glassy Polymers, Applied Science Publishers LTD, London.

James F. Carley, 1991. "Modern Plastics Encyclopedia '91" McGraw-Hill, Inc. N. J.

Jelinski, L. W., J. J. Dumais, R. E. Stark, T. S. Ellis, and F. E. Karasz, 1983. Macromolecules, 16, 1019.

Jin, X., T.S. Ellis, and F.E. Karasz, 1984. J. Polym. Sci. Polym. Phys. Edi., Vol. 22, 1701-1717.

Kawasaki, K., Y. Sekita and K. Kanou, 1962. J. Clloid Sci. 17, 865

Lebovits, A. 1966. Permeability of Polymers to gases, Vapors and Liquids. Modern Plastics. 43:139.

Langmuir, I., J., 1918. Am. Chem. Soc., 40, 1361.

Meares, 1954.

Meares, P., 1958. Trans. Faraday Soc., 54, 40-6.

Meares, P., 1958a. Diffusion of Allyl Chloride in PVA. Part I. The Steady State of Permeation. J. Polym. Sci. 27, 391.

Meares, P., 1958b. Diffusion of Allyl Chloride in PVA. Part II. The Transient State of Permeation. J. Polym. Sci. 27, 405.

Meares, P., 1965. "Polmers: Structure and Bulk Properties". Van Nostrand & Co. LTD, London.

Michaels, A. and Bixler, H., 1961. J. Polym. Sci. 50, 413-39.

Michaels, A. and Parker, R., 1959. J. Polym. Sci., 41, 54-71.

Michaels, A., Vieth, W. and Barrrie, J., 1963. J. Appl. Phys., 34(1), 1.

Moy, P. and Karasz, F. E, 1980. Water in Polymers, Am. Chem. Soc. Symp. Ser. 127, S. P. Rowland, Ed., American Chemical Society, Washington, DC.

Myers, A. W., Rogers, C. E., Stannett, V. and Szwarc, M., 1958. Tappi, 41, 716.

Nielson, Lawrence E., 1974. "Mechanical properties of polymers and composites". Vol. 1. Marcel Dekker Publishing Co.,

Onogi, S., K. Sasaguri, T. Adachi, and S. Ogihara, 1962. J. Polym. Sci. 58,1.

Papir, Y. S., S. Kapur, C. E. Rogers, and E. Baer, 1972. J. Polym. Sci. Part A-2 Vol. 10, 1305-1319.

Prausnitz, J. M., R. N. Lichtenthale and E. Gomez de Azevedo, 1986. "Molecular Thermodynamics of Fluid-Phase Equilibria, 2nd Ed., Prentice-Hall, Inc., N. J.

Puffr, R. and Sabenda, J., 1967. On the Structure and Properties of Polyamides: XXVII. The Sorption of Water In Polyamides. J. Polym. Sci. Part C, 16, 79-93.

Quistwater, J. M. R., and B. A. Dunell, 1958. J. Polym. Sci. 1, 267.

Quistwater, J. M. R., and B. A. Dunell, 1959. J. Apply. Polym. Sci. 58, 1.

Rogers, C. E., 1964. Permeability and Chemical Resistance of Polymers. ch 9. in "Engineering Design for Plastics". Baer, E. (ed). Rheinhold, N. Y.

Rogers, C. E., V. Stannett, and M. Szwarc, 1960. The Sorption, Diffusion and Permeation of Organic Vapors In Polyethylene. J. Polym. Sci. 45, 61.

Satton, W. O., 1967. J. Polymer Science, 18C, 33.

Sauer, J. A. and T. Lim, 1977. J. Macromol. Sci. Phys., B13, 419.

Sfirakis A., and Rogers, C. E., 1980. Polym. Eng. Sci., 20(4), 294.

Starkweather, H. W., 1973. "Nylon Plastics". John Wiley & Sons, N. Y.

Starkweather, H. W., G. E. Moore, J. E. Hansen, T. M. Roder, and R. E. Brrks, 1956. J. Polym. Sci. 21, 189.

Tobolsky, A. V., 1960. "Properties and Structure of Polymers". J. Wiley and Sons, Inc., New York.

Vieth, W. R., J. M. Howell and J. H. Hsieh, 1976. J. Membrane Sci., 1, 177.

Wunderlich, B., and Cromier, 1967. J. Polymer Science, A-2, 5, 987.

Yang, D. K., W. J. Koros, H. B. Hopfenberg and V. T. Stannett, 1985. J. Appl. Polym. Sci. Sorption and Transport Studies of Water in Kapton Polyamide I, 30, 1035.